ACS Catalysis

pubs.acs.org/acscatalysis

Research Article

# Transition-State Stabilization by Secondary Orbital Interactions between Fluoroalkyl Ligands and Palladium During Reductive Elimination from Palladium(aryl)(fluoroalkyl) Complexes

Eric D. Kalkman,[†] Yehao Qiu,[†] and John F. Hartwig*

Cite This: *ACS Catal.* 2023, 13, 12810−12825

Read Online

ACCESS | Metrics & More | Article Recommendations | Supporting Information



**ABSTRACT:** Palladium-catalyzed fluoroalkylations of aryl halides are valuable reactions for the synthesis of fluorinated, biologically active molecules. Reductive elimination from an intermediate Pd(aryl)(fluoroalkyl) complex is the step that forms the C(aryl)−C(fluoroalkyl) bond, and this step typically requires higher temperatures and proceeds with slower rates than the reductive elimination of nonfluorinated alkylarenes from the analogous Pd(aryl)(alkyl) complexes. The experimental rates of this step correlate poorly with common parameters, such as the steric property or the electron-withdrawing ability of the fluoroalkyl ligand, making the prediction of rates and the rational design of Pd-catalyzed fluoroalkylations difficult. Therefore, a systematic study of the features of fluoroalkyl ligands that affect the barrier to this key step, including steric properties, electron-withdrawing properties, and secondary interactions, is necessary for the future development of fluoroalkylation reactions that occur under milder conditions and that tolerate additional types of fluoroalkyl reagents. We report computational studies of the effect of the fluoroalkyl ($R^F$) ligand on the barriers to reductive elimination from Pd(aryl)($R^F$) complexes ($R^F$ = $CF_2CN$, $CF_2C(O)Me$, etc.) containing the bidentate ligand di-*tert*-butyl(2-methoxyphenyl)phosphine (**L**). The computed Gibbs free-energy barriers to reductive elimination from these complexes suggest that fluoroalkylarenes should form quickly at room temperature for the fluoroalkyl ligands we studied, excluding $R^F$ = $CF_3$, $CF_2Me$, $C_2F_5$, $CF_2CFMe_2$, $CF_2Et$, $CF_2iPr$, or $CF_2tBu$. Analyses of the transition-state structures by natural bond orbital (NBO) and independent gradient model (IGMH) approaches reveal that orbital interactions between the Pd center and a hydrogen atom or $\pi$-acid bonded to the $\alpha$-carbon atom of the $R^F$ ligand stabilize the lowest-energy transition states of Pd(aryl)($R^F$) complexes. Comparisons between conformers of transition-state structures suggest that the magnitude of such stabilizations is 4.7−9.9 kcal/mol. In the absence of these secondary orbital interactions, a more electron-withdrawing fluoroalkyl ligand leads to a higher barrier to reductive elimination than a less electron-withdrawing fluoroalkyl ligand. Computations on the reductive elimination from complexes containing *para*-substituted aryl groups on palladium reveal that the barriers to reductive elimination from complexes containing more electron-rich aryl ligands tend to be lower than those to reductive elimination from complexes containing less electron-rich aryl ligands when the fluoroalkyl ligands of these complexes can engage in secondary orbital interactions with the metal center. However, the computed barriers to reductive elimination do not depend on the electronic properties of the aryl ligand when the fluoroalkyl ligands do not engage in secondary orbital interactions with the metal center.

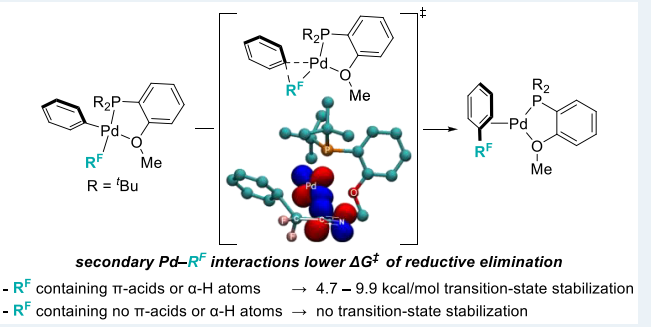


**KEYWORDS:** *fluoroalkylation, palladium catalysis, reductive elimination, DFT calculations, secondary orbital interactions*

## INTRODUCTION

The construction of organic molecules containing fluorine is important for the development of biologically active compounds, including pharmaceuticals and agrochemicals, because fluorinated functional groups alter the lipophilicity, acidity, and metabolic stability of these molecules.[1−10] Pd-catalyzed fluoroalkylations of aryl halides are attractive reactions to introduce fluorinated motifs at late stages of synthesis because of the high selectivity and functional-group tolerance of Pd catalysts (Scheme 1a).[11] The C−C bond-forming step of these catalytic fluoroalkylation reactions is reductive elimination from an intermediate palladium(aryl)(fluoroalkyl) complex to form a fluoroalkylarene. While the reductive elimination step is not always rate-limiting in the catalytic reactions,[12,13] the reductive elimination of fluoroalkylarenes, nevertheless, is often much slower than the reductive

Received: June 9, 2023
Revised: September 1, 2023
Published: September 18, 2023

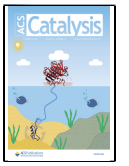

**Scheme 1**

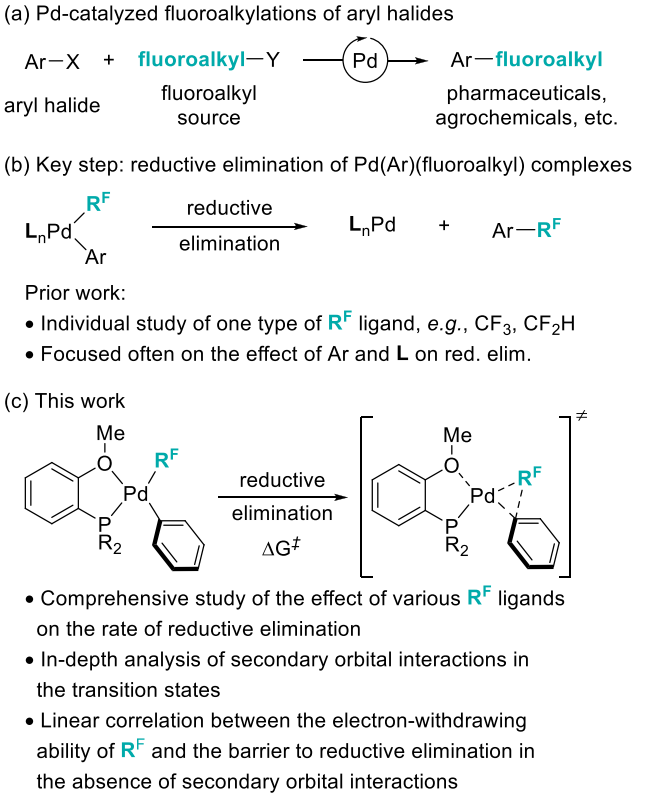


elimination of nonfluorinated alkylarenes from analogous palladium(aryl)(alkyl) complexes.[11,14−16] As such, the rate of this step imposes an upper bound on the rate of the reaction overall and affects the partitioning of the reaction between the steps on the catalytic cycle and those occurring off the cycle to form side products or induce the decomposition of the catalyst. Thus, understanding how structural and electronic effects of the Pd(aryl)(fluoroalkyl) complexes affect the rate of reductive elimination is key for the development of new, milder Pd-catalyzed fluoroalkylation reactions.

Many experimental and computational studies on the reductive elimination from Pd complexes containing perfluoroalkyl, difluoromethyl, and $\alpha$-fluoroenolate ligands have been reported.[15−33] However, most of these studies have focused on a single fluoroalkyl ligand, e.g., the $CF_3$ group and have not compared this reductive elimination to those involving other fluoroalkyl or nonfluorinated alkyl ligands (Scheme 1b). A comparison of reductive elimination from complexes containing various types of fluoroalkyl ligands would provide insight into structural and electronic properties that influence the rate of the reductive elimination step and aid the future development of Pd-catalyzed fluoroalkylations of aryl halides (Scheme 1c).

To this end, we report computational investigations into the reductive elimination of fluoroalkylarenes from (**L**)Pd(aryl)($R^F$) complexes (**L** = di-*tert*-butyl(2-methoxyphenyl)-phosphine) containing a series of alkyl and fluoroalkyl ligands $R^F$ ($R^F$ = $CF_3$, $C_2F_5$, $CF_2H$, $CF_2CH_3$, $CF_2CF(CH_3)_2$, $CFH_2$, $CH_3$, $CF_2Ph$, $CF_2CN$, $CF_2C(O)F$, $CF_2C(O)H$, $CF_2C(O)Me$, $CF_2CO_2Me$, $CHFC(O)Me$, $CF_2Et$, $CF_2iPr$, or $CF_2tBu$), leading to new insights into the factors controlling reductive elimination. We find that the barriers to reductive elimination from complexes of fluoroalkyl ligands containing electron-withdrawing $\pi$-acids (carbonyl, nitrile, or aryl moieties) or hydrogen atoms attached to the $\alpha$-carbon are significantly lower than those from complexes of fluoroalkyl ligands that do not contain these moieties. Analyses of these structures by natural bond orbital (NBO) analysis[34] and the independent gradient model based on Hirshfeld partition (IGMH)[35−37] reveal that the lower barriers for the complexes containing $\pi$-acids or $\alpha$-hydrogens result from the stabilizing secondary orbital interactions between the Pd center and the $\pi$-acidic or $\alpha$-hydrogen substituents in the fluoroalkyl ligand.

## RESULTS AND DISCUSSION

**Validation of the Computational Methods.** All optimized structures and their corresponding energies were calculated using the Gaussian 16 software package[38] at the PBE0-D3(BJ)/ma-TZVP/def2-QZVP(Pd)//PBE0-D3(BJ)/def2-SVP/def2-TZVP(Pd) level of theory[39−42] in THF or toluene solvent according to the SMD model[43] (see the

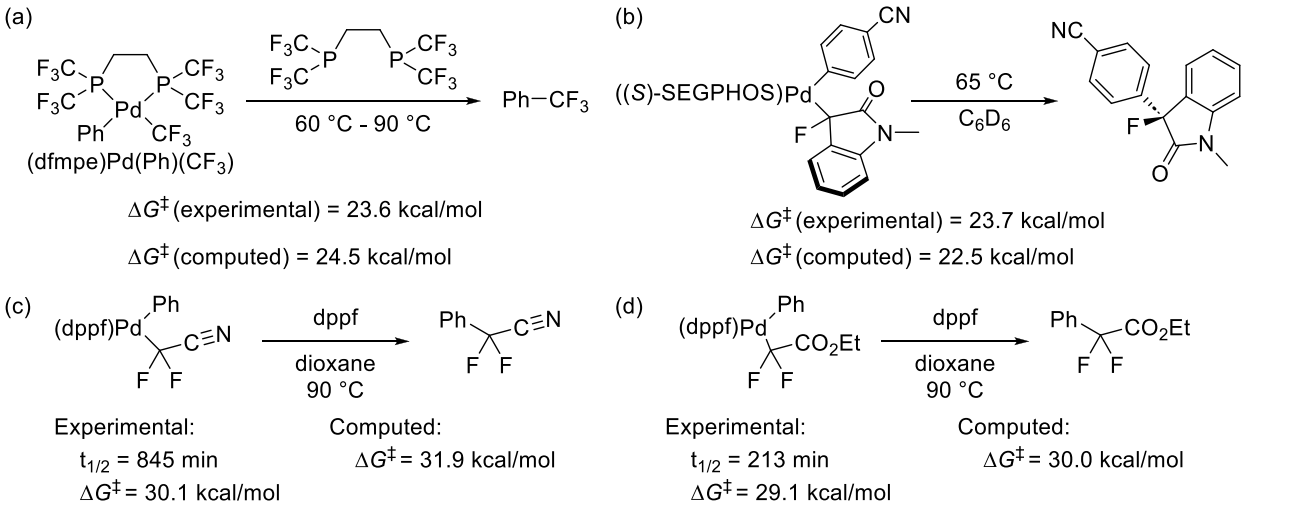


**Figure 1.** Comparison of experimentally determined and computed barriers to reductive elimination from (a) (dfmpe)Pd(Ph)($CF_3$),[24] (b) ((*S*)-SEGPHOS)Pd(4-CN-$C_6H_4$)(fluorooxindole),[12] (c) (dppf)Pd(Ph)($CF_2CN$), and (d) (dppf)Pd(Ph)($CF_2CO_2Et$).[15]



https://doi.org/10.1021/acscatal.3c02648
ACS Catal. 2023, 13, 12810−12825

**Scheme 2. Reported Pd-Catalyzed Aryldifluoromethylation of Aryl Halides and the Model System Studied in This Work**

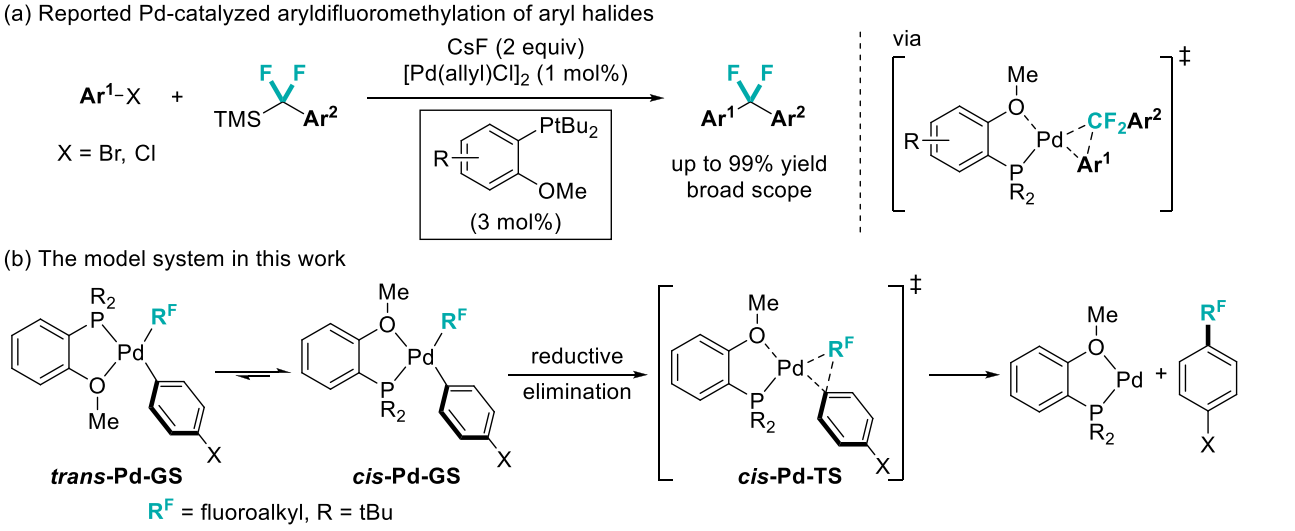


Supporting Information for additional details). The computational methods chosen for this work closely reproduce higher-level computations of closed-shell organometallic complexes in established DFT benchmarks[44−46] as well as experimentally determined energetic barriers to reductive elimination from arylpalladium fluorooxindole complexes.[12] Nevertheless, we calculated the barriers to reductive elimination from Pd complexes containing various bisphosphine ligands and fluoroalkyl groups and compared the computed barriers to those derived from published experimental measurements.[12,15,24] The barrier to reductive elimination from the complex (dfmpe)Pd(Ph)($CF_3$) (dfmpe = 1,2-bis(bis-(trifluoromethyl)phosphino)ethane) reported by Schoenebeck and co-workers was calculated to be 24.5 kcal/mol, which is only 0.9 kcal/mol higher than the value measured from experiments (Figure 1(a)).[24] This difference is similar to that between computed and experimental barriers to reductive elimination from the (aryl)Pd(fluorooxindole) complex containing the (*S*)-SEGPHOS ligand (1.2 kcal/mol, Figure 1(b)) that we published previously.[12] Similarly, the computed barriers to reductive elimination from (dppf)Pd(phenyl)-(fluoroalkyl) complexes (dppf = 1,1′-bis(diphenylphosphino)-ferrocene) agree with experimental values (Figure 1(c) and (d), $|\Delta G^{\ddagger}_{calc} - \Delta G^{\ddagger}_{expt}| < 1.8$ kcal/mol).[15] The calculated barrier to reductive elimination from (dppf)Pd(Ph)($CF_2CN$) was 1.9 kcal/mol higher than that from (dppf)Pd(Ph)($CF_2CO_2Et$) ($\Delta G^{\ddagger}_{calc}(CF_2CN) - \Delta G^{\ddagger}_{calc}(CF_2CO_2Et)$ = 1.9 kcal/mol), consistent with barriers calculated from experimentally determined rate constants ($\Delta G^{\ddagger}_{expt}(CF_2CN) - \Delta G^{\ddagger}_{expt}(CF_2CO_2Et)$ = 1.0 kcal/mol).[15] These small differences between computation and experiment show that our computational method accurately predicts the relative free-energy barriers to reductive elimination from Pd(aryl)(fluoroalkyl) complexes.

**Geometries and Energies of Optimized Structures.** Having confirmed that our computational method accurately predicts the barriers to reductive elimination from Pd(aryl)-(fluoroalkyl) complexes, we investigated the effect of the identity of the fluoroalkyl ligand on the barrier to reductive elimination. We selected Pd complexes containing the aryldialkylphosphine ligand di-*tert*-butyl(2-methoxyphenyl)-phosphine (**L**) as the model system because our group recently showed that Pd complexes containing **L** catalyzed the aryldifluoromethylation of aryl halides with high yields and a broad scope (Scheme 2(a)).[32,47] Other aryldialkylphoshines containing alkoxyaryl moieties such as BrettPhos, RuPhos, and SPhos also have been reported to facilitate a variety of Pd-catalyzed fluoroalkylation reactions;[13,18,48] however, we did not investigate systems containing these ligands due to their large sizes and accompanying high computational costs.

We optimized the ground-state and transition-state geometries of a series of palladium complexes **Pd-R$^F$** in THF solvent (eq 1, *trans*- or *cis*-**Pd-R$^F$-GS** and *trans*- or *cis*-**Pd-R$^F$-TS**, respectively). The calculated relative Gibbs free energies ($\Delta G$) and selected geometric parameters of representative **Pd-R$^F$** structures are shown in Table 1 (see Table 2 below and Table S1 in the Supporting Information for the data of all other **Pd-R$^F$** structures). Structures in which the fluoroalkyl ligand was either *cis* to the methoxy fragment of the ligand **L** (*cis*-**Pd-R$^F$**) or *trans* to it (*trans*-**Pd-R$^F$**) were considered (Figure 2(a) and (c), respectively, R$^F$ = $CF_2Ph$ as an example); in most cases, the ground-state free energy of the *cis* isomer was lower than that of the *trans* isomer ($\Delta G_{trans} - \Delta G_{cis}$ = 0.2−2.1 kcal/mol). The exception was the system in which R$^F$ = $CF_2H$; in this case, the *trans* isomer was slightly more stable ($\Delta G_{trans} - \Delta G_{cis}$ = −0.3 kcal/mol). Both *cis* and *trans* ground-state complexes adopted slightly distorted square-planar structures, with $\varphi$ = 170−180°, in which $\varphi$ is defined as the dihedral angle formed by C(Ph)−Pd−P−O or C(R$^F$)−Pd−P−

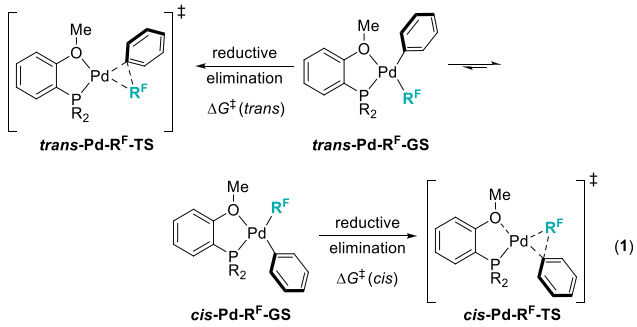


R = tBu; R$^F$ = $CF_3$, $C_2F_5$, $CF_2H$, $CF_2CH_3$, $CFH_2$, $CH_3$, $CF_2CFMe_2$, $CF_2CN$, $CF_2Ph$, $CF_2C(O)F$, $CF_2C(O)H$, $CF_2C(O)Me$, $CF_2CO_2Me$, $CHFC(O)Me$, $CF_2iPr$, $CF_2tBu$



https://doi.org/10.1021/acscatal.3c02648
ACS Catal. 2023, 13, 12810−12825

Table 1. Calculated Relative Gibbs Free Energies ($\Delta G$) and Selected Geometric Parameters of the Lowest-Energy Ground-State and Transition-State Structures of Representative *cis*- and *trans*-Pd-$R^F$ Complexes

| $R^F$ | structure | $\Delta G$ (kcal/mol) | $r$ (Pd−P) (Å) | $r$ (Pd−O) (Å) | $\varphi$ (C(Ph),Pd, P, O) (°) | $\varphi$ (C($R^F$),Pd, P, O) (°) |
|---|---|---|---|---|---|---|
| $CF_3$ | *cis*-GS | 0.0 | 2.39 | 2.29 | 175 | |
| | *cis*-TS | 28.2 | 2.33 | 2.47 | 176 | |
| | *trans*-GS | 1.1 | 2.40 | 2.29 | | 176 |
| | *trans*-TS | 27.3 | 2.34 | 2.54 | | 178 |
| $CF_2CN$ | *cis*-GS | 0.0 | 2.36 | 2.29 | 179 | |
| | *cis*-TS | 21.0 | 2.34 | 2.77 | 147 | |
| | *trans*-GS | 2.1 | 2.40 | 2.30 | | 179 |
| | *trans*-TS | 24.7 | 2.38 | 2.53 | | 173 |
| $CF_2Ph$ | *cis*-GS | 0.0 | 2.39 | 2.31 | 171 | |
| | *cis*-TS | 17.3 | 2.33 | 2.92 | 123 | |
| | *trans*-GS | 0.2 | 2.40 | 2.32 | | 180 |
| | *trans*-TS | 23.0 | 2.37 | 2.61 | | 176 |
| $CF_2H$ | *cis*-GS | 0.3 | 2.40 | 2.29 | 176 | |
| | *cis*-TS | 18.5 | 2.34 | 2.66 | 156 | |
| | *trans*-GS | 0.0 | 2.39 | 2.29 | | 176 |
| | *trans*-TS | 19.7 | 2.35 | 2.58 | | 180 |
| $CFH_2$ | *cis*-GS | 0.0 | 2.39 | 2.30 | 173 | |
| | *cis*-TS | 16.0 | 2.33 | 2.60 | 154 | |
| | *trans*-GS | 1.5 | 2.37 | 2.31 | | 172 |
| | *trans*-TS | 17.2 | 2.35 | 2.57 | | 174 |
| $CH_3$ | *cis*-GS | 0.0 | 2.37 | 2.30 | 180 | |
| | *cis*-TS | 14.0 | 2.33 | 2.59 | 166 | |
| | *trans*-GS | 1.1 | 2.36 | 2.31 | | 177 |
| | *trans*-TS | 15.6 | 2.35 | 2.57 | | 178 |
| $CF_2C(O)Me$ | *cis*-GS | 0.0 | 2.40 | 2.30 | 173 | |
| | *cis*-TS | 21.6 | 2.35 | 2.72 | 140 | |
| | *trans*-GS | 1.8 | 2.39 | 2.30 | | 179 |
| | *trans*-TS | 23.2 | 2.38 | 2.54 | | 175 |
| $CF_2C(O)H$ | *cis*-GS | 0.0 | 2.40 | 2.31 | 175 | |
| | *cis*-TS | 20.6 | 2.37 | 2.74 | 133 | |
| | *trans*-GS | 1.0 | 2.38 | 2.31 | | 178 |
| | *trans*-TS | 20.1 | 2.38 | 2.51 | | 176 |

O for *cis* or *trans* complexes, respectively (Figure 2(a) and (c), $R^F$ = $CF_2Ph$ as an example). In these computed ground-state structures, the distances from the Pd center to the phosphine and the methoxy fragment of the bidentate ligand **L** ($r$(Pd−P) = 2.36−2.41 Å and $r$(Pd−O) = 2.27−2.32 Å, respectively) were in close agreement with values obtained from reported crystal structures of similar (**L**)Pd complexes ($r$(Pd−P) = 2.29−2.32 Å and $r$(Pd−O) = 2.27−2.30 Å, respectively).[49,50]

The lowest-energy transition-state structures for reductive elimination from the *cis* and *trans* complexes (*cis*- and *trans*-**Pd-$R^F$-TS**) were also computed. As was the case for the ground-state structures, the transition-state geometries were calculated to be lower in energy for the *cis* structures than for the *trans* structures for most fluoroalkyl ligands ($\Delta G^{\ddagger}_{trans} - \Delta G^{\ddagger}_{cis}$ = 0.7−5.7 kcal/mol). Exceptions to this trend were complexes with $R^F$ = $CF_3$, $C_2F_5$, and $CF_2C(O)H$, for which the *trans* transition-state structures were slightly lower in energy than the *cis* analogs ($\Delta G^{\ddagger}_{trans} - \Delta G^{\ddagger}_{cis}$ = −0.9, −0.1, and −0.5 kcal/mol, respectively). The Pd−O bonds in the transition-state structures *trans*-**Pd-$R^F$-TS** were moderately longer than those in the ground states ($\Delta r$(Pd−O) = 0.2−0.3 Å), and the degrees of distortion from square planar in the transition states were only slightly larger ($|\Delta\varphi| < 6°$) than those in the ground states (Table 1 and Figure 2(d)). In contrast, larger changes in the structures were computed to occur during the reductive elimination from the *cis*-**Pd-$R^F$** isomers. As the reaction proceeds from *cis*-**Pd-$R^F$-GS** to *cis*-**Pd-$R^F$-TS**, the methoxy fragment of the ligand **L** twists significantly out of the plane defined by other ligated groups on the Pd center (Table 1 and Figure 2(b)), the Pd−O bond lengthens ($\Delta r$(Pd−O) = 0.2−0.6 Å), and the deviation from the square-planar geometry ($\Delta\varphi$ = 14−48° except for $R^F$ = $CF_3$ ($\Delta\varphi$ = −1°)) is larger than it is during reductive elimination from the *trans*-**Pd-$R^F$** isomers. These changes in structure suggest that the Pd−O bond is weaker in transition state *cis*-**Pd-$R^F$-TS** than in *trans*-**Pd-$R^F$-TS**. We note that a similar elongation of the Pd−O bond in the transition state was observed in a previous DFT study on the reductive elimination from alkylpalladium amido complexes containing similar methoxy-substituted aryldialkylphosphine ligands.[50] We hypothesized that the greater degree of dissociation of the methoxy substituent on the ligand in *cis*-**Pd-$R^F$-TS**, relative to that of the same group in the ancillary ligand of *trans*-**Pd-$R^F$-TS**, might reduce the destabilizing steric interaction of the methoxy group with the adjacent migrating $R^F$ ligand and allow for stabilizing interactions between the $R^F$ ligand and the Pd center (*vide infra*), ultimately leading to lower barriers to reductive elimination.

Overall, the calculated barriers indicate that reductive elimination from 10 of the 17 **Pd-$R^F$** complexes studied would proceed quickly even at 25 °C ($\Delta G^{\ddagger} \leq 22.3$ kcal/mol, corresponding to a predicted $t_{1/2}$ < 45 min for $R^F \neq CF_3$, $C_2F_5$, $CF_2Me$, $CF_2Et$, $CF_2iPr$, $CF_2tBu$, or $CF_2CFMe_2$). The seven


https://doi.org/10.1021/acscatal.3c02648
ACS Catal. 2023, 13, 12810−12825

Table 2. $Q(R^F)$ Values for the Fluoroalkyl Ligands $R^F$ and Calculated Free Energies Related to the Reductive Elimination of *cis*-Pd-$R^F$ Complexes[a]

| $R^F$ | $Q(R^F)$ | $\Delta G^{\ddagger}(R^F)$ (kcal/mol) | $\Delta G^{\ddagger}_{rot}(R^F)$ (kcal/mol) | $\Delta\Delta G^{\ddagger}(R^F)$ (kcal/mol) | $\Delta E_{orb}(R^F)$ (kcal/mol) | $\Delta G^{\ddagger}_{no\text{-}orb}(R^F)$ (kcal/mol) |
|---|---|---|---|---|---|---|
| $CF_2CN$ | −0.492 | 21.0 | 33.1 | −12.1 | −9.9 | 30.9 |
| $CF_2Ph$ | −0.402 | 17.3 | 28.4 | −11.1 | −6.9 | 24.2 |
| $CF_2H$ | −0.370 | 18.2 | 25.1 | −6.9 | −4.7 | 22.9 |
| $CF_2C(O)Me$ | −0.438 | 21.6 | 30.7 | −9.1 | −6.6 | 28.2 |
| $CF_2C(O)H$ | −0.455 | 20.6 | 29.5 | −8.9 | −6.6 | 27.2 |
| $CF_2CO_2Me$ | −0.442 | 22.3 | 30.9 | −8.6 | −4.7 | 27.0 |
| $CF_2C(O)F$ | −0.491 | 21.9 | 32.1 | −10.1 | −7.9 | 29.8 |
| $C_2F_5$[b] | −0.478 | 28.9 | 31.3 | −2.5 | n/a | 28.9 |
| $CF_2Me$[b] | −0.377 | 23.3 | 25.5 | −2.2 | n/a | 23.3 |
| $CF_2Et$[b] | −0.359 | 24.3 | 26.5 | −2.2 | n/a | 24.3 |
| $CF_2iPr$[b] | −0.359 | 24.0 | 29.2 | −5.1 | n/a | 24.0 |
| $CF_2tBu$[b] | −0.370 | 24.1 | 28.2 | −4.2 | n/a | 24.1 |
| $CF_2CFMe_2$[b] | −0.414 | 25.7 | 29.5 | −3.8 | n/a | 25.7 |
| $CF_3$[bc] | −0.462 | 28.2 | n/a | n/a | n/a | 28.2 |
| $CFH_2$[d] | −0.321 | 16.0 | not found | n/a | n/a | n/a |
| $CH_3$[c] | −0.292 | 14.0 | n/a | n/a | n/a | n/a |
| $CFHC(O)Me$[c] | −0.426 | 20.6 | not found | n/a | n/a | n/a |

[a]Definitions of energetic terms: $\Delta G^{\ddagger}(R^F)$, the barrier to reductive elimination involving the lowest-energy transition state *cis*-**Pd-$R^F$-TS**; $\Delta G^{\ddagger}_{rot}(R^F)$, the barrier to reductive elimination involving the transition states *cis*-**Pd-$R^F$-TS-rot**, in which the $\alpha$-H or the $\alpha$-$\pi$-acceptor is oriented away from the Pd center; $\Delta\Delta G^{\ddagger}(R^F) = \Delta G^{\ddagger}(R^F) - \Delta G^{\ddagger}_{rot}(R^F)$; $\Delta E_{orb}(R^F) = \Delta\Delta G^{\ddagger}(R^F) - \Delta E_{se}(R^F)$, the energy attributable to solely secondary orbital interactions, where $\Delta E_{se}(R^F)$ is the estimated energetic penalty attributed to changing steric and electronic interactions caused by the rotation of the $R^F$ ligand (see Table 4); $\Delta G^{\ddagger}_{no\text{-}orb}(R^F) = \Delta G^{\ddagger}(R^F) - \Delta E_{orb}(R^F)$, the estimated barrier for the hypothetical scenario in which secondary orbital interactions are absent in the *cis*-**Pd-$R^F$-TS** structures. [b]Since these $R^F$ ligands do not engage in secondary orbital interactions with the Pd center in *cis*-**Pd-$R^F$-TS** structures, $\Delta G^{\ddagger}(R^F) = \Delta G^{\ddagger}_{no\text{-}orb}(R^F)$ by definition. [c]Due to the symmetric nature of these $R^F$ ligands, the *cis*-**Pd-$R^F$-TS-rot** structures are identical to the *cis*-**Pd-$R^F$-TS** structures. Therefore, analysis based on $\Delta G^{\ddagger}_{rot}(R^F)$ is not applicable to these structures. [d]We were unable to locate the transition-state structures *cis*-**Pd-$R^F$-rot** in which the $\alpha$-hydrogens or the $\alpha-\pi$-acceptor were oriented away from the Pd for these $R^F$ ligands. Therefore, we have omitted analyses of $\Delta G^{\ddagger}_{rot}(R^F)$ for these structures.

exceptions are **Pd-$CF_3$**, **Pd−$C_2F_5$**, **Pd-$CF_2Me$**, **Pd-$CF_2Et$**, **Pd-$CF_2iPr$**, **Pd-$CF_2tBu$**, and **Pd-$CF_2CFMe_2$**. The computed barriers to reductive elimination from these seven Pd complexes suggest that reductive elimination would be slow at room temperature and proceed at a reasonable rate only at elevated temperatures. The half-lives for reductive elimination from complexes containing the ligands $R^F$ = $CF_2Me$, $CF_2Et$, $CF_2iPr$, $CF_2tBu$, and $CF_2CFMe_2$ would be 3, 15, 9, 11, and 120 min, respectively, at 60 °C, while those for reductive elimination from complexes with $R^F$ = $CF_3$ and $C_2F_5$ would be 49 and 125 min, respectively, at 100 °C. These computational results are consistent with the high temperatures required in experimental work for reductive elimination from related monophosphine-ligated aryl(perfluoroalkyl)palladium complexes to form perfluoroalkylarenes.[13,18,19,22]

**Quantification of the Electronic Properties of Fluoroalkyl Ligands and Analysis of the Features of Fluoroalkyl Ligands that Affect the Barriers to Reductive Elimination.** To determine the factors that affect the barriers to reductive elimination, we first quantitatively assessed the effect of the electronic properties of the fluoroalkyl ligands on the Gibbs free energy of activation ($\Delta G^{\ddagger}$). It was not possible simply to compare $\Delta G^{\ddagger}$ values to the Hammett substituent constants of the $R^F$ ligands of *cis*-**Pd-$R^F$** structures,[51] as was done in previous studies on the reductive eliminations from arylpalladium thiolate,[52] amide,[53] and alkoxide species,[54,55] because of the lack of published substituent constants for several of the $R^F$ ligands. Thus, we developed a new descriptor for the electronic properties of $R^F$ ligands: $Q(R^F)$, which is the sum of the QTAIM atomic charges[56,57] of the fluoroalkyl ($R^F$) fragment in the ground-state structures *cis*-**Pd-$R^F$-GS** (Scheme 3, $R^F$ = $CF_2CN$ as an example).[58] For a comparison of $Q(R^F)$ to descriptors based on other atomic charge schemes, we refer the reader to section 3 of the Supporting Information. We reasoned that a more electron-withdrawing $R^F$ fragment in the ground-state complex *cis*-**Pd-$R^F$-GS** would contain a greater share of the electron density of the molecule, leading to a more negative $Q(R^F)$ value. To evaluate this new descriptor, we plotted the $Q(R^F)$ values of the difluoroalkyl ($R^F$ = $CF_2X$) ligands against the $\sigma_m$ substituent constant of the X group, a parameter commonly used to quantify inductive effects in linear free-energy relationships (Figure 3).[59,60] The strong linear correlation ($R^2$ = 0.96) between $Q(CF_2X)$ and $\sigma_m(X)$ demonstrates that $Q(R^F)$ does reflect quantitatively the electron-withdrawing properties of the $R^F$ ligands.

We next plotted the free-energy barriers to reductive elimination ($\Delta G^{\ddagger}$) from the *cis*-**Pd-$R^F$** complexes against the $Q(R^F)$ values of the $R^F$ fragments (Figure 4 and Table 2). A high degree of scatter can be seen in this plot when all data points are considered ($R^2$ = 0.248, Figure 4(a)). For example, the $Q(R^F)$ values and, hence, the electron-withdrawing abilities of $R^F$ = $C_2F_5$ and $R^F$ = $CF_2CN$ are similar ($Q(C_2F_5)$ = −0.478 and $Q(CF_2CN)$ = −0.492), but the barrier to reductive elimination from *cis*−**Pd-$C_2F_5$** is 7.9 kcal/mol higher than the corresponding barrier to elimination from *cis*-**Pd-$CF_2CN$** ($\Delta G^{\ddagger}(C_2F_5)$ = 28.9 kcal/mol and $\Delta G^{\ddagger}(CF_2CN)$ = 21.0 kcal/mol). Likewise, the $Q(R^F)$ values of $R^F$ = $CF_2Me$ and $R^F$ = $CF_2H$ are similar ($Q(CF_2Me)$ = −0.377 and $Q(CF_2H)$ = −0.370), but the barrier to reductive elimination from *cis*-**Pd-$CF_2Me$** is 5.1 kcal/mol higher than that from *cis*-**Pd-$CF_2H$** ($\Delta G^{\ddagger}(CF_2Me)$ = 23.3 kcal/mol and $\Delta G^{\ddagger}(CF_2H)$ = 18.2 kcal/mol). Thus, the barriers to reductive elimination depend on more than the $Q(R^F)$ values alone.


https://doi.org/10.1021/acscatal.3c02648
ACS Catal. 2023, 13, 12810−12825

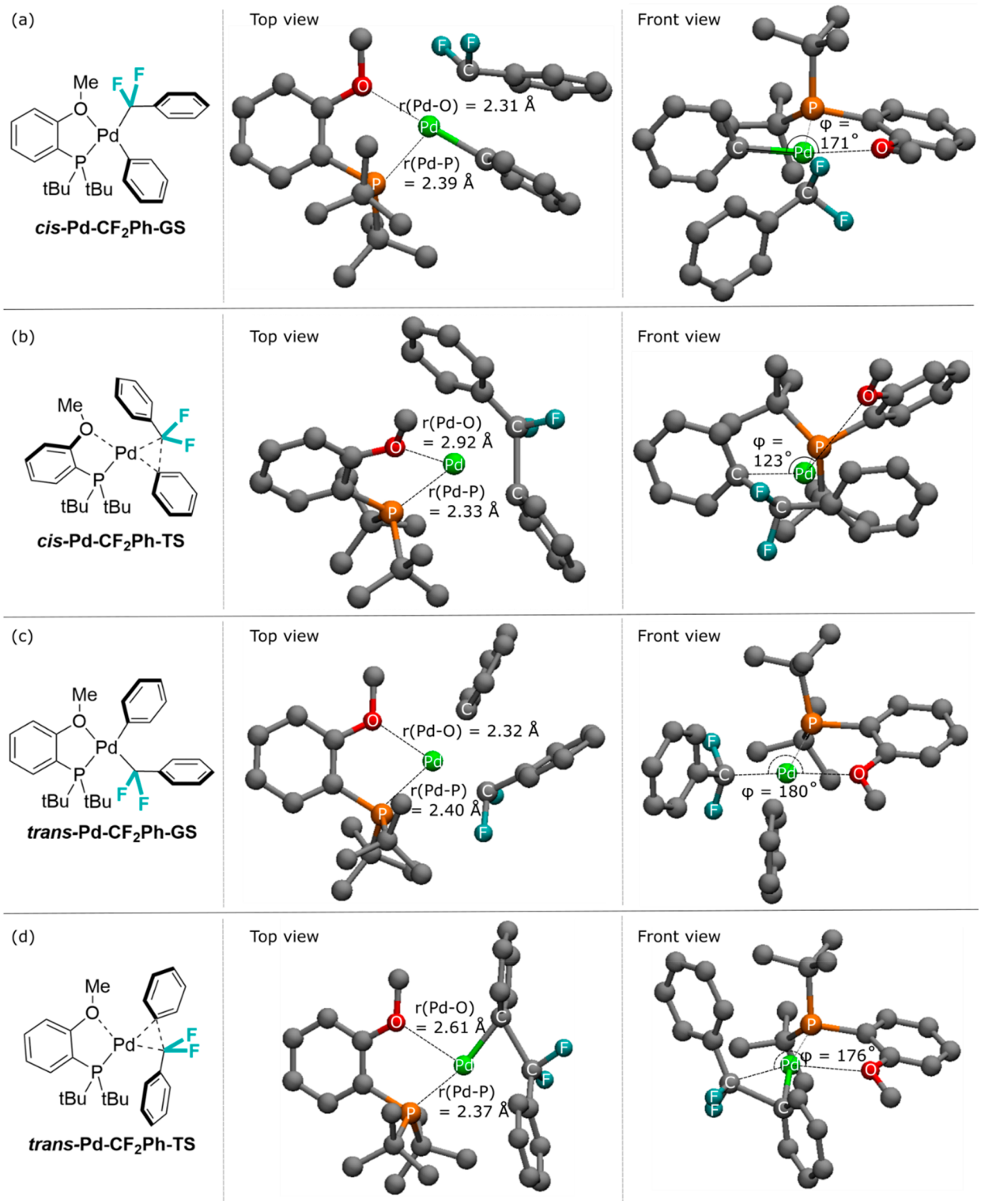


**Figure 2.** Optimized structures and selected geometric parameters of (a) *cis*-**Pd-CF$_2$Ph-GS**, (b) *cis*-**Pd-CF$_2$Ph-TS**, (c) *trans*-**Pd-CF$_2$Ph-GS**, and (d) *trans*-**Pd-CF$_2$Ph-TS**. Hydrogen atoms have been omitted for clarity.

We recently suggested that a donor−acceptor interaction between the d orbitals of Pd and a $\pi^*$ orbital of the $R^F$ fragment was present in the transition states for reductive elimination from aryl(3-fluorooxindolyl)- and aryl-(difluoromethylaryl)palladium complexes.[12,47] Thus, we hypothesized that the lack of correlation between $\Delta G^{\ddagger}(R^F)$ and $Q(R^F)$ could result from the presence or absence of such interactions within *cis*-**Pd-TS-R$^F$** complexes containing different $R^F$ ligands. Indeed, the data points can be partitioned into two subsets that individually correlate $\Delta G^{\ddagger}(R^F)$ more strongly with $Q(R^F)$: a lower-energy subset **A** ($R^2$ = 0.831), in which the $R^F$ ligands contain unsaturated groups or hydrogen atoms attached to the $\alpha$-carbon atom (Figure 4(b), orange triangles), and a higher energy subset **B** ($R^2$ = 0.932), in which the $R^F$


https://doi.org/10.1021/acscatal.3c02648
ACS Catal. 2023, 13, 12810−12825

**Scheme 3. Illustration of the Definition of $Q(R^F)$ Using $R^F$ = $CF_2CN$ as an Example**[a]

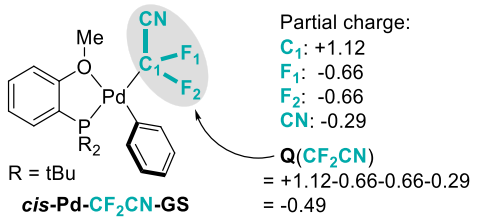


[a]$Q(CF_2CN)$ is equal to the sum of the QTAIM partial charge of each atom of the $CF_2CN$ fragment in the lowest-energy ground-state structure *cis*-**Pd-$CF_2CN$-GS**.

ligands are saturated and do not contain $\alpha$-hydrogen atoms (Figure 4(b), blue squares). Within each subset, the correlation between $\Delta G^{\ddagger}(R^F)$ and $Q(R^F)$ is negative, indicating that the barriers to reductive elimination from aryl(fluoroalkyl)palladium complexes containing more electron-withdrawing fluoroalkyl ligands are higher than those containing less electron-withdrawing fluoroalkyl ligands, a trend that matches the well-established trend for reductive eliminations from arylpalladium complexes containing non-fluorinated alkyl ligands.[16,61−63]

**Analysis of the Stabilizing Secondary Orbital Interactions between Pd and the Fluoroalkyl Ligands in the Transition States of Subset A.** Further analysis of metal−ligand bonding in the ground and transition states provides strong evidence that the two subsets lie on distinct correlation lines because the transition states of subset **A** are stabilized by secondary orbital interactions between Pd and an unsaturated group or an $\alpha$-hydrogen atom in the fluoroalkyl ligand, but the transition states of subset **B** are not. The fluoroalkyl ligands in the transition states for reductive elimination from the complexes in subset **A** are oriented such that the $\pi^*$ orbitals of the electrophilic aryl, nitrile, or carbonyl groups ($R^F$ = $CF_2Ph$, $CF_2CN$, and $CF_2C(O)R$) can interact with the Pd center (Figure 5). To determine whether bonding interactions are present in such structures, we conducted IGMH (independent gradient model based on Hirshfeld partition)[35−37] and NBO (natural bond orbital)[34] analyses of these transition-state structures. IGMH analysis classifies interactions in specific regions of molecular space and assigns colors to these regions based on whether the interactions are

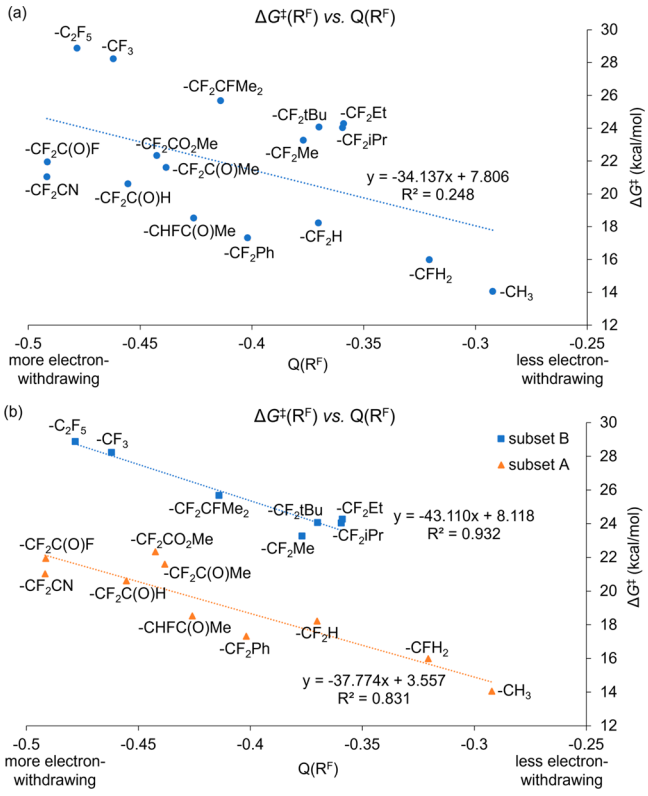


**Figure 4.** Plots of computed barriers to reductive elimination ($\Delta G^{\ddagger}(R^F)$) against $Q(R^F)$ values (a) without partitioning of $R^F$ ligands into subsets and (b) with partitioning of $R^F$ ligands into subsets.

attractive and stabilizing (blue), repulsive and destabilizing (red), or the result of van der Waals interactions (green). The IGMH plots of transition-state structures *cis*-**Pd-$R^F$-TS** possessing unsaturated groups in the $R^F$ fragments clearly contain blue isosurfaces between the Pd center and the $sp^2$ or sp carbon in the carbonyl, nitrile, or phenyl groups (indicated by black arrows in Figure 5(a)(ii), (b)(ii), and (c)(ii); $R^F$ = $CF_2C(O)Me$, $CF_2CN$, and $CF_2Ph$, respectively), indicating stabilizing, bonding-like interactions between them. Furthermore, second-order NBO analysis, which determines the presence of stabilizing interactions by electron donation from filled NBOs into vacant acceptor NBOs, reveals a stabilizing

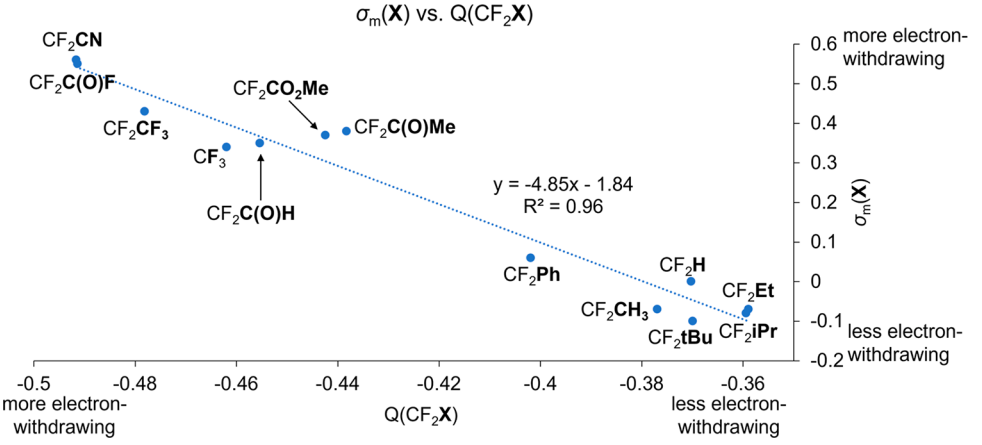


**Figure 3.** Linear relationship between the $Q(CF_2X)$ and the $\sigma_m(X)$ values for a series of difluoroalkyl ligands.



https://doi.org/10.1021/acscatal.3c02648
ACS Catal. 2023, 13, 12810−12825

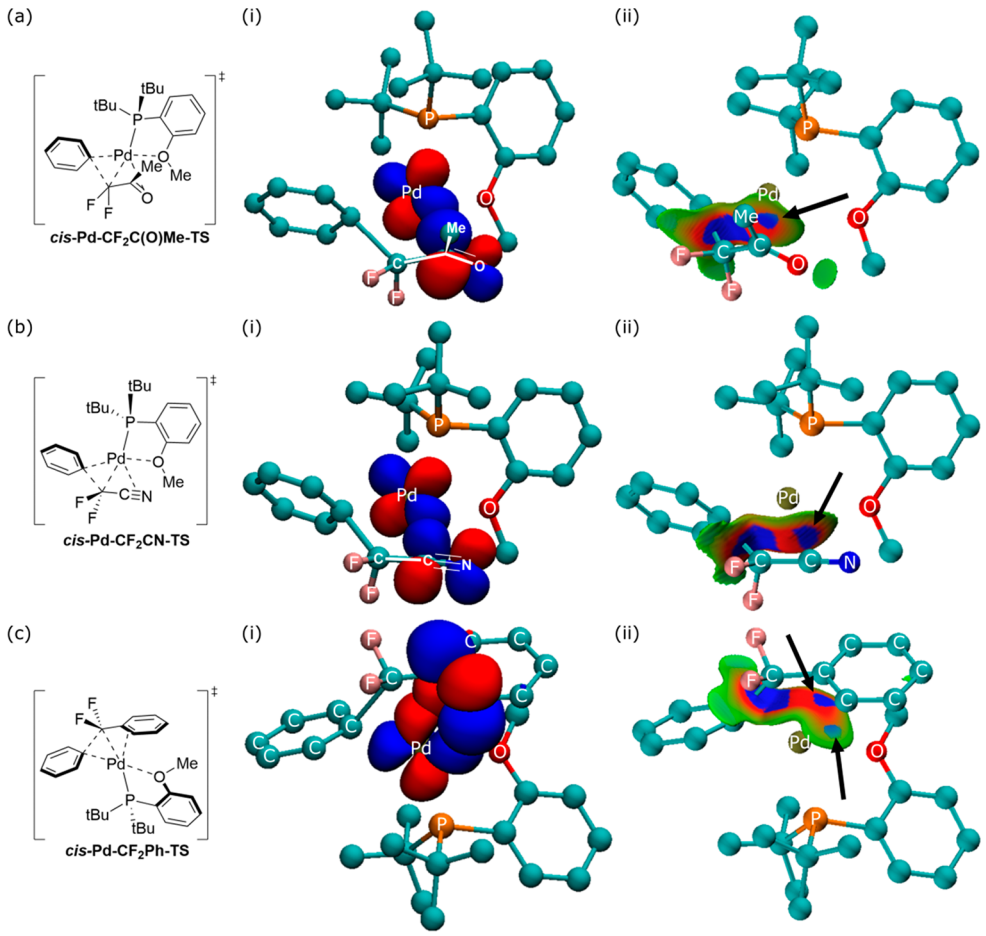


**Figure 5.** NBO and IGMH analyses of the stabilizing secondary orbital interactions in *cis*-**Pd-R$^F$-TS** structures between the Pd center and (a) the $\alpha$-carbonyl group for $R^F$ = $CF_2C(O)Me$, (b) the $\alpha$-nitrile group for $R^F$ = $CF_2CN$, and (c) the $\alpha$-phenyl group for $R^F$ = $CF_2Ph$. NBO isosurfaces depict the leading orbitals involved in the $d(Pd) \rightarrow \pi^*(R^F)$ interactions. Blue isosurfaces labeled with black arrows in the IGMH plots indicate stabilizing interactions between the $R^F$ ligand and the Pd center.

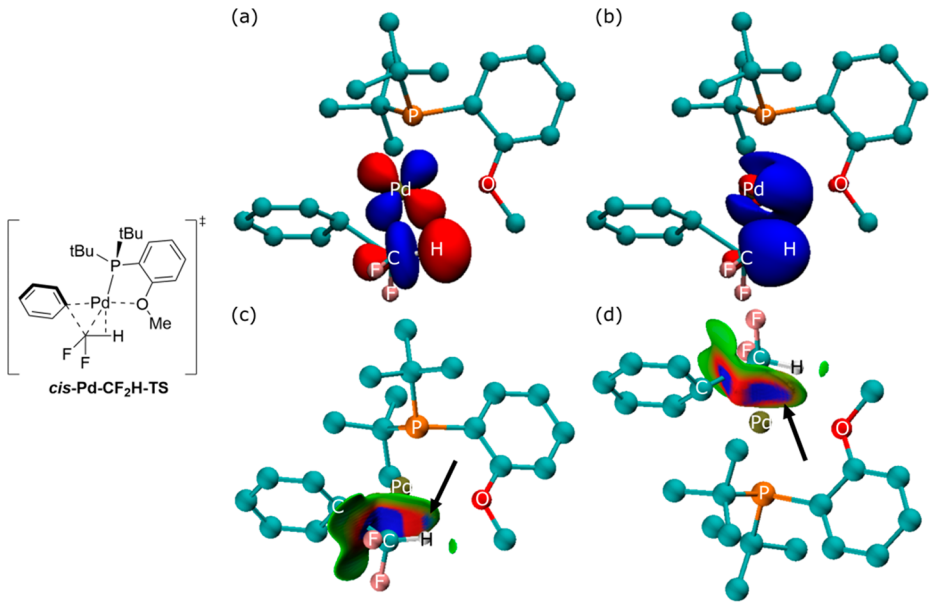


**Figure 6.** NBO and IGMH analyses of the stabilizing secondary orbital interactions between the Pd center and the C($\alpha$)−H bond in the transition state *cis*-**Pd-$CF_2$H-TS**. (a) Visualization of the $d(Pd) \rightarrow \sigma^*(C-H)$ orbital interaction. (b) Visualization of the $\sigma(C-H) \rightarrow s(Pd)$ orbital interaction. (c and d) IGMH plots; blue isosurfaces labeled with black arrows indicate stabilizing interactions between the $R^F$ ligand and the Pd center.



https://doi.org/10.1021/acscatal.3c02648
ACS Catal. 2023, 13, 12810−12825

donor−acceptor interaction from a mostly filled d orbital of the Pd center into the mostly vacant $\pi^*$ orbitals of the carbonyl, nitrile, and phenyl fragments (Figure 5(a)(i), (b)(i), and (c)(i), respectively).

A similar examination of the structures of *cis*-**Pd-R$^F$-TS** for R$^F$ = $CH_3$, $CFH_2$, $CF_2H$, and CHFC(O)Me reveals that the $\alpha$-C−H bond is oriented so that the $\sigma$ and $\sigma^*$ orbitals of the C−H bond interact with the Pd center (Figure 6, R$^F$ = $CF_2H$ as an example). IGMH plots of the transition states contain blue regions between the Pd atom and the $\alpha$-hydrogen atom of the methyl or fluoroalkyl ligands, suggesting the presence of stabilizing interactions between them (Figure 6(c) and (d)). NBO analysis reveals two stabilizing interactions between the C−H bond and the Pd center in these transition-state structures: (1) a stabilizing donor−acceptor interaction from a mostly filled d orbital of the Pd center into the mostly vacant $\sigma^*$ orbital of the C−H bond (Figure 6(a)) and (2) a stabilizing donor−acceptor interaction from the mostly filled $\sigma$ orbital of the C−H bond to the mostly vacant 5s orbital of the Pd center (Figure 6(b)). Similar C−H agostic interactions also have been proposed to be present in the transition states for reductive eliminations from Pt(IV) and Pd(IV) methyl complexes[64,65] and are in agreement with early theoretical studies on reductive elimination reactions.[66,67] These results support our hypothesis that transition states in subset **A** containing unsaturated groups or $\alpha$-hydrogens in the R$^F$ ligands are stabilized by secondary orbital interactions between the Pd center and the $\pi$-accepting groups or the $\alpha$-hydrogens.

Analysis of the Wiberg bond indices[68] (calculated in the NAO basis) between Pd and the $\pi$-acid or the $\alpha$-hydrogen in the structures lying on the intrinsic reaction coordinates (IRCs) for reductive elimination from *cis*-**Pd-R$^F$** complexes in subset **A** suggests that the Pd···H and the Pd···$\pi^*$ interactions are absent in the lowest-energy ground-state structures *cis*-**Pd-R$^F$-GS**. Therefore, these interactions are specific to the transition states. Figures 7(a) and (b) show the Wiberg bond index between Pd and the cyano group as well as the index between Pd and $\alpha$-H along the reaction coordinates for the reductive elimination from *cis*-**Pd-$CF_2$CN** and *cis*-**Pd-$CF_2$H** complexes (as representative examples for Pd···$\pi^*$ and Pd···H interactions, respectively). In the reactive complex, which is similar in structure to the lowest-energy ground state, the bond index between Pd and the substituent in the fluoroalkyl ligand is small (0.072 for Pd···CN and less than 0.02 for Pd···H), suggesting that the bonding interactions between the metal and the substituent in the R$^F$ fragment are absent. As the reaction progresses to the transition state, the bond index between Pd and the substituent increases (Pd···CN, from 0.072 to 0.278; Pd···H, from <0.02 to 0.0412), indicating the emergence of orbital interactions between the metal and the $\pi$-acceptor or the $\alpha$-hydrogen in the transition state. After the C−C bond has formed between the phenyl and $CF_2CN$ fragments, the phenyl ring moves farther from the Pd center, whereas the cyano group moves closer to the metal, leading to a larger Wiberg bond index between Pd and CN in the product than in the transition state (Figure 7(a)). In contrast, after the C−C bond has formed between the phenyl and difluoromethyl fragments, the C($sp^3$)−H bond rotates away from the Pd, resulting in a smaller bond index between Pd and H in the product than in the transition state (Figure 7(b)). Although the bond index in the product may be smaller or larger than that in the transition state depending on the identity of the R$^F$ ligand, such changes in this bonding

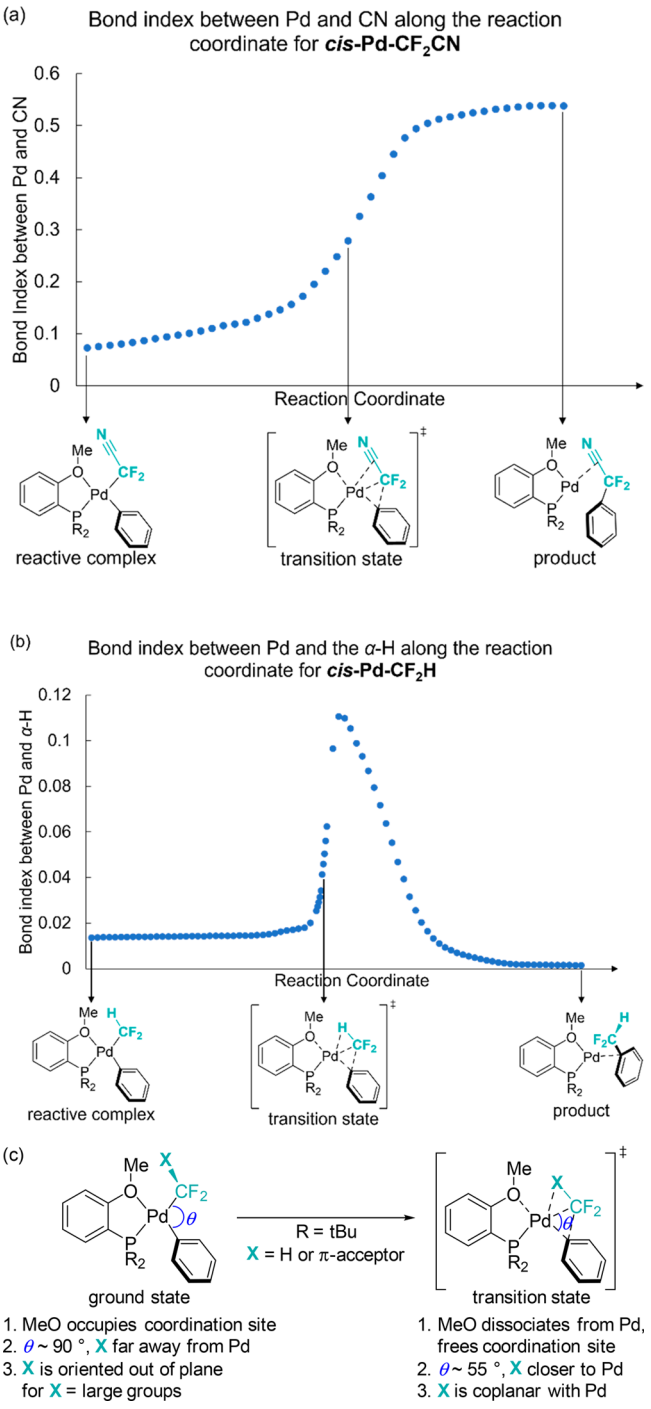


**Figure 7.** (a) Wiberg bond index between Pd and CN along the reaction coordinate for the reductive elimination from the *cis*-**Pd-$CF_2$CN** complex. (b) Wiberg bond index between Pd and $\alpha$-H along the reaction coordinate for the reductive elimination from the *cis*-**Pd-$CF_2$H** complex. (c) Rationalizations for why secondary orbital interactions are specific to the transition states.

interaction occur after the transition state and, therefore, do not affect our analysis of the orbital interactions in the ground state versus the transition state. The small Wiberg bond indices between the metal and the substituent in the fluoroalkyl ligand in the reactive complexes versus the significantly larger bond indices in the transition states strongly suggest that the stabilizing secondary orbital interactions are specific to the


https://doi.org/10.1021/acscatal.3c02648
ACS Catal. 2023, 13, 12810−12825

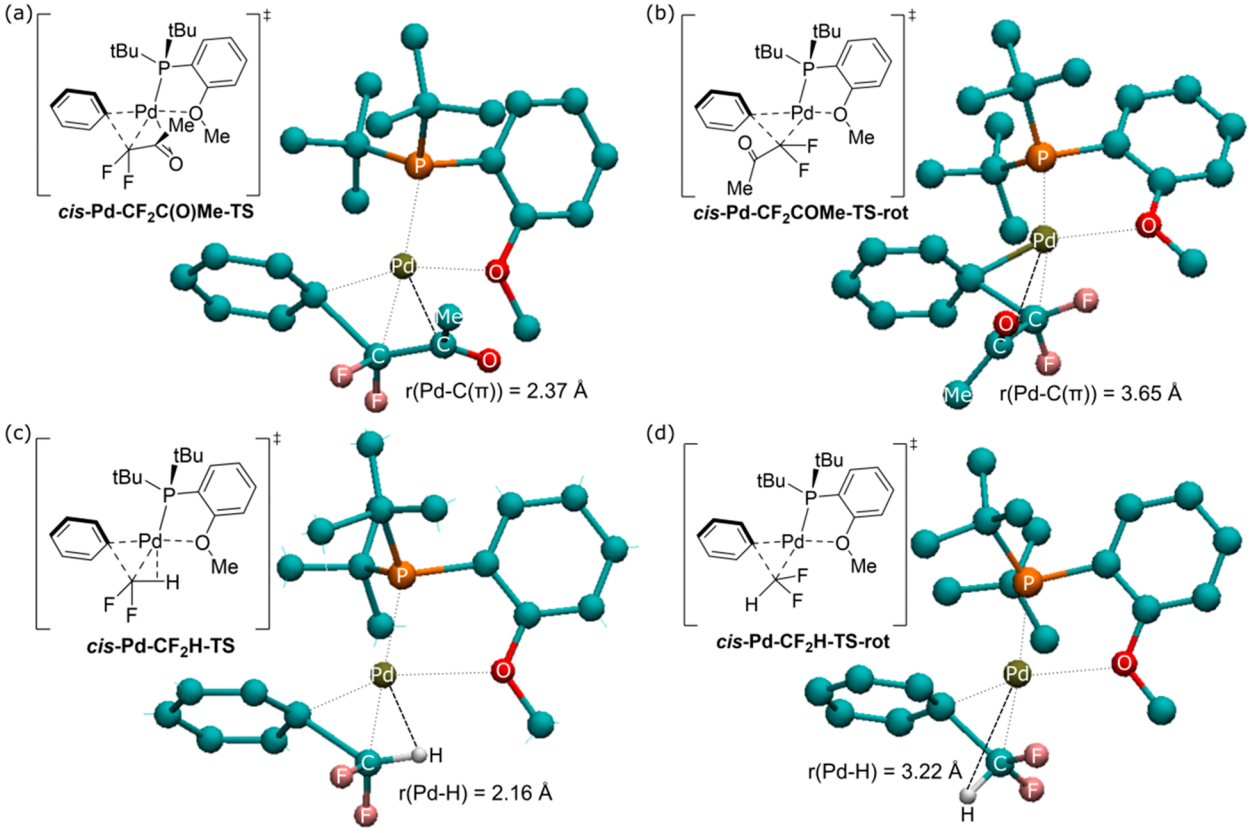


**Figure 8.** Optimized transition-state structures of (a) *cis*-**Pd-CF$_2$C(O)Me-TS**, (b) *cis*-**Pd-CF$_2$C(O)Me-TS-rot**, (c) *cis*-**Pd-CF$_2$H-TS**, and (d) *cis*-**Pd-CF$_2$H-TS-rot**.

**Table 3. Distances between the Pd Center and the $\alpha$-H or the Electrophilic Atom of the $\alpha$-$\pi$-Acid in Optimized Transition-State Structures *cis*-Pd-R$^F$-TS and *cis*-Pd-R$^F$-TS-rot**

| entry | R$^F$ | $r$(Pd···X)[a] in *cis*-**Pd-R$^F$-TS** (Å) | $r$(Pd···X)[a] in *cis*-**Pd-R$^F$-TS-rot** (Å) | $r_{vdW}$(Pd) + $r_{vdW}$(X)[a] (Å)[69] |
|---|---|---|---|---|
| 1 | $CF_2CN$ | 2.22 | 3.64 | 3.33 |
| 2 | $CF_2C(O)Me$ | 2.37 | 3.65 | |
| 3 | $CF_2C(O)H$ | 2.24 | 3.63 | |
| 4 | $CF_2CO_2Me$ | 2.41 | 3.66 | |
| 5 | $CF_2C(O)F$ | 2.30 | 3.66 | |
| 6 | $CF_2Ph$ | 2.29 | 3.66 | |
| 7 | $CF_2H$ | 2.16 | 3.22 | 2.83 |

[a]X refers to the atom that is $\alpha$ to the difluoromethylene moiety. X = H($\alpha$) for R$^F$ = $CF_2H$; X = C($\pi$) for any other R$^F$.

transition-state structures and, therefore, influence the free-energy barriers to reductive elimination.

We propose that the secondary orbital interactions are absent in the ground-state structures *cis*-**Pd-R$^F$-GS** for the following reasons: (1) the distance between Pd and the methoxy fragment of ligand **L** is short and the coordination site on the metal is occupied; (2) the bond angle $\theta$ formed by C(R$^F$)−Pd−C(Ph) is close to 90°, so the distance between Pd and the substituent in the fluoroalkyl ligand is long; and (3) the $\pi$-acceptor lies out of the plane defined by the atoms bound to Pd in complexes containing large R$^F$ ligands due to steric repulsions (Figure 7(c), left). In contrast, the secondary orbital interactions can be present in the transition states *cis*-**Pd-R$^F$-TS** because (1) the methoxy group of ligand **L** dissociates from the metal center to open a coordination site; (2) the R$^F$ ligand migrates closer to the phenyl ligand as the reaction proceeds, decreasing the bond angle $\theta$ (from ∼90° to ∼55°) and the distance between Pd and the $\pi$-acceptor or the $\alpha$-H; and (3) the substituent in the migrating fluoroalkyl ligand is coplanar with the Pd center, enabling favorable overlap between the orbitals. All of these factors lead to the presence of stabilizing orbital interactions between Pd and the fluoroalkyl ligand in the transition state but not in the ground state.

**Determination of the Energetic Stabilizations Resulting from Secondary Orbital Interactions.** Having identified features in the R$^F$ ligands that engage in secondary orbital interactions with the Pd center as well as the causes for such stabilizations, we sought to estimate the energetic stabilization resulting from these features. To do so, we compared the *cis*-**Pd-R$^F$-TS** structures to higher-energy transition-state structures in which the stabilizing groups of the fluoroalkyl ligand were oriented away from the Pd center by rotation about the Pd−R$^F$ bond (*cis*-**Pd-R$^F$-TS-rot**) (Figure 8). The free energies of the *cis*-**Pd-R$^F$-TS-rot** structures, relative to those of the corresponding ground-state structures


https://doi.org/10.1021/acscatal.3c02648
ACS Catal. 2023, 13, 12810−12825

**Table 4. Calculated Volumes of Protonated Fluoroalkyl Fragments and Estimates of the Energetic Penalties ($\Delta E_{se}$) Associated with Reorienting the $R^F$ Ligands in the *cis*-Pd-$R^F$-TS-rot Structures**

| $R^F_B$ | calculated volume of $R^F_B$ (Å$^3$)[a] | $\Delta E_{se}(R^F_B) = \Delta\Delta G^{\ddagger}(R^F_B)$ (kcal/mol) | $R^F_A$ | calculated volume of $R^F_A$ (Å$^3$)[a] | $\Delta E_{se}(R^F_A)$ (kcal/mol) |
|---|---|---|---|---|---|
| $CF_2Me$ | 75.5 | −2.2 | $CF_2CN$ | 76.1 | −2.2 |
| $C_2F_5$ | 90.6 | −2.5 | $CF_2CO_2Me$ | 111.6 | −3.9 |
| $CF_2Et$ | 98.5 | −2.2 | $CF_2C(O)F$ | 82.5 | −2.3 |
| $CF_2iPr$ | 121.1 | −5.1 | $CF_2C(O)H$ | 78.3 | −2.3 |
| $CF_2CFMe_2$ | 125.8 | −3.8 | $CF_2C(O)Me$ | 100.8 | −2.5 |
| $CF_2tBu$ | 143.0 | −4.2 | $CF_2H$ | 52.0 | −2.2[b] |
| | | | $CF_2Ph$ | 148.7 | −4.2[b] |

[a]See the Supporting Information for calculations of the volumes of $R^F$ fragments. [b]$\Delta E_{se}$ values of $R^F_A$ ligands whose volumes lie outside the range of the volumes of the $R^F_B$ ligands were assigned to the $\Delta E_{se}$ value of the $R^F_B$ ligand closest in size.

of ***cis*-Pd-$R^F$-GS** ($\Delta G^{\ddagger}_{rot}(R^F)$), are reported in Table 2, and representative geometries for ***cis*-Pd-$R^F$-TS** and ***cis*-Pd-$R^F$-TS-rot** are compared in Figure 8 ($R^F$ = $CF_2H$ and $CF_2CN$ as examples) and Table 3. By separating the Pd center from the unsaturated groups or $\alpha$-hydrogen atoms of the $R^F$ ligand, we reasoned that the secondary orbital interactions would be much weaker or absent. Indeed, in the rotameric transition-state structures ***cis*-Pd-$R^F$-TS-rot**, the distances between the Pd center and the $\alpha$-hydrogen or the $\alpha$-$\pi$-acid are greater than the sum of the van der Waals radii of the corresponding atoms (Table 3), demonstrating that the Pd center does not interact directly with the $\alpha$-hydrogen or the $\alpha$-$\pi$-acid in the $R^F$ ligand.

The energies of ***cis*-Pd-$R^F$-TS-rot** are higher than those of ***cis*-Pd-$R^F$-TS** by 6.9−12.1 kcal/mol for the complexes of $R^F$ in subset **A** and by 2.2−5.1 kcal/mol for the complexes of $R^F$ in subset **B** (Table 2). We recognize that the difference in energy between ***cis*-Pd-$R^F$-TS** and ***cis*-Pd-$R^F$-TS-rot** ($\Delta\Delta G^{\ddagger}(R^F)$) does not arise solely from the aforementioned donor−acceptor interactions ($\Delta E_{orb}(R^F)$). Other differences in the steric and electronic properties ($\Delta E_{se}(R^F)$) caused by the rotation of the $R^F$ fragment exist between these two structures. Thus, we decomposed $\Delta\Delta G^{\ddagger}(R^F)$ into a term representing the stabilization energy arising from the secondary orbital interactions ($\Delta E_{orb}(R^F)$) and a term representing the energetic penalty resulting from other differences between the steric and electronic properties of the structures ($\Delta E_{se}(R^F)$). That is,

$$\Delta\Delta G^{\ddagger}(R^F) = \Delta G^{\ddagger}(R^F) - \Delta G^{\ddagger}_{rot}(R^F) = \Delta E_{orb}(R^F) + \Delta E_{se}(R^F) \quad (2)$$

To estimate $\Delta E_{se}(R^F)$, we first considered that $\Delta E_{se}(R^F) = \Delta\Delta G^{\ddagger}(R^F)$ for $R^F$ ligands that did *not* participate in donor−acceptor orbital interactions (i.e., those in subset **B**: $R^F_B$ = $C_2F_5$, $CF_2CH_3$, $CF_2Et$, $CF_2iPr$, $CF_2tBu$ and $CF_2CFMe_2$, for which $\Delta E_{orb}(R^F_B) = 0$; see Table 2). Then, we reasoned that $\Delta E_{se}(R^F)$ values would be similar for $R^F$ ligands of similar sizes (see the Supporting Information for details regarding the volumes of $R^F$ ligands) and estimated the $\Delta E_{se}(R^F_A)$ values by interpolating the $\Delta E_{se}(R^F_B)$ values with respect to the volumes of the $R^F$ ligands[70] (Table 4). By solving eq 2 for $\Delta E_{orb}$, we obtained a quantitative estimate of the magnitude of the stabilizing secondary orbital interactions, $\Delta E_{orb}(R^F)$, in transition state ***cis*-Pd-$R^F$-TS** for each $R^F$ ligand (eq 3). From this analysis, we determined that the secondary orbital interactions stabilized the lowest-energy transition states to reductive elimination by 4.7−9.9 kcal/mol (Table 2, column $\Delta E_{orb}(R^F)$).

$$\Delta E_{orb}(R^F) = \Delta\Delta G^{\ddagger}(R^F) - \Delta E_{se}(R^F) \quad (3)$$

$$\Delta\Delta G^{\ddagger}_{no\text{-}orb}(R^F) = \Delta G^{\ddagger}(R^F) - \Delta E_{orb}(R^F) \quad (4)$$

Subtracting $\Delta E_{orb}(R^F)$ from the barrier to reductive elimination corresponding to the lowest-energy transition state ($\Delta G^{\ddagger}(R^F)$) affords the new parameter $\Delta G^{\ddagger}_{no\text{-}orb}(R^F)$ (eq 4), which estimates the hypothetical barrier to reductive elimination through the lowest-energy transition-state structure ***cis*-Pd-$R^F$-TS** in the absence of secondary orbital interactions between the Pd center and the $R^F$ ligand. By plotting the $\Delta G^{\ddagger}_{no\text{-}orb}(R^F)$ values versus the $Q(R^F)$ values, we observed that subsets **A** and **B** no longer constitute distinct groups. Instead, these new transition-state barriers for all complexes together correlate well with the corresponding $Q(R^F)$ values (Figure 9, $R^2$ = 0.910). Thus, in the absence of

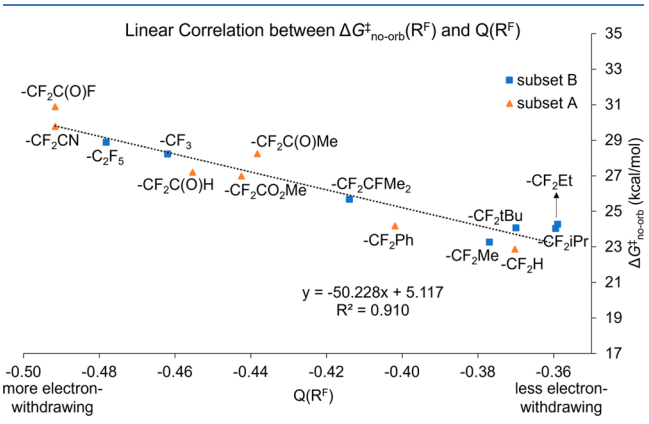


**Figure 9.** Linear correlation between $\Delta G^{\ddagger}_{no\text{-}orb}(R^F)$ and $Q(R^F)$. $\Delta G^{\ddagger}_{no\text{-}orb}(R^F)$ is the estimated hypothetical barrier to reductive elimination through the lowest-energy transition-state structure ***cis*-Pd-$R^F$-TS** in the absence of secondary orbital interactions between the Pd center and the $R^F$ ligand; "no-orb" stands for "no orbital".

secondary orbital interactions, complexes of more electron-withdrawing fluoroalkyl ligands generally undergo reductive elimination more slowly than those with less electron-withdrawing fluoroalkyl ligands, and this result is consistent with general trends for reductive elimination from palladium(alkyl)(aryl) complexes in which complexes containing more electron-withdrawing alkyl ligands undergo reductive elimination to form alkylarenes more slowly than complexes containing less electron-withdrawing alkyl ligands.[16,61−63] Furthermore, the absence of the distinction between subsets **A** and **B** after the secondary orbital stabilizations are removed strongly suggests that these orbital interactions are the primary,


https://doi.org/10.1021/acscatal.3c02648
ACS Catal. 2023, 13, 12810−12825

**Table 5. Comparison of Reductive Elimination from Palladium(phenyl)(fluoroalkyl) Complexes Containing the Hemilabile Ligand L and the Nonlabile Bisphosphine Ligand L′**

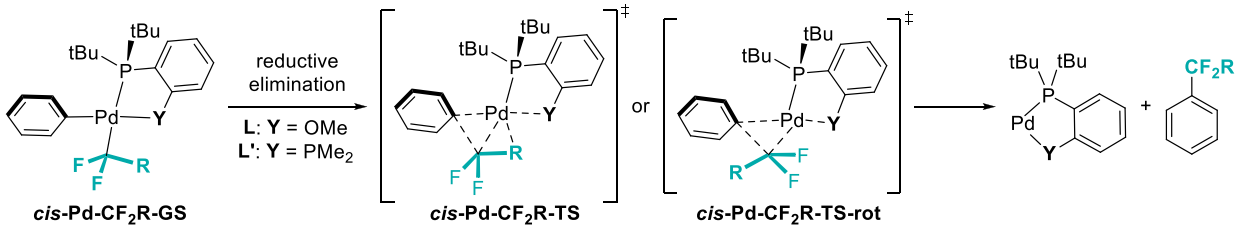


| | ligand = L (Y = OMe) | | | ligand = L′ (Y = $PMe_2$) | | |
|---|---|---|---|---|---|---|
| $CF_2R$ | $\Delta G^{\ddagger}$(L, $R^F$) (kcal/mol) | $\Delta G^{\ddagger}_{rot}$(L, $R^F$) (kcal/mol) | $\Delta E_{orb}$(L, $R^F$) (kcal/mol) | $\Delta G^{\ddagger}$(L′, $R^F$) (kcal/mol) | $\Delta G^{\ddagger}_{rot}$(L′, $R^F$) (kcal/mol) | $\Delta E_{orb}$(L′, $R^F$) (kcal/mol)[a] |
| $CF_2H$ | 18.2 | 25.1 | −4.7 | 31.0 | 33.9 | −0.6 |
| $CF_2CN$ | 21.0 | 33.1 | −9.9 | 32.7 | 41.5 | −6.5 |
| $CF_2Ph$ | 17.3 | 28.4 | −6.9 | 30.8 | 38.3 | −3.3 |

[a]Estimated using the $\Delta E_{se}(R^F)$ values found in Table 4 for Y = OMe.

if not the sole, features distinguishing subset **A** from subset **B**. Indeed, a comparison of the barriers to reductive eliminations from Pd complexes containing $R^F$ ligands with similar $Q(R^F)$ values but varying sizes ($R^F$ = $CF_2Me$, $CF_2Et$, $CF_2iPr$, and $CF_2tBu$) suggests that any additional steric effect of $R^F$ ligands on the barriers is small ($\Delta G^{\ddagger}$ = 23.3−24.3 kcal/mol; see section 5 of the Supporting Information for a more detailed discussion).

**Effect of the Hemilabile Ligand on the Secondary Orbital Interactions.** As illustrated in Figure 7(c), dissociation of the methoxy group of ligand **L** from the Pd center in transition state *cis*-**Pd-$R^F$-TS** accompanies the secondary orbital interactions. To investigate the impact of this dissociation on the stabilization from these secondary interactions, we computed the barriers to reductive elimination from palladium(phenyl)(fluoroalkyl) complexes (fluoroalkyl = $CF_2H$, $CF_2CN$, and $CF_2Ph$) containing the nonlabile bisphosphine ligand **L′** (**L′** = di-*tert*-butyl(2-dimethylphosphinophenyl)phosphine) and compared the results to those for reductive elimination from (**L**)Pd(aryl)(fluoroalkyl) complexes (Table 5). The barriers to reductive elimination from (**L′**)Pd complexes are significantly higher than those from (**L**)Pd complexes ($\Delta G^{\ddagger}$(L′, $R^F$) − $\Delta G^{\ddagger}$(L, $R^F$) = 11.7−13.5 kcal/mol). This difference in barrier is consistent with the well-established trend that reductive elimination from three-coordinate complexes is faster than that from closely related four-coordinate complexes.[71] At the same time, this study shows that the stabilization from secondary orbital interactions in the transition states for reductive elimination from (**L′**)Pd complexes is smaller than that from (**L**)Pd complexes ($|\Delta E_{orb}$(L, $R^F$)| − $|\Delta E_{orb}$(L′, $R^F$)| = 3.4−4.1 kcal/mol; see the Supporting Information for calculation details). Such differences in energy suggest that dissociation of the methoxy fragment of the hemilabile ligand **L** in the transition state enhances the stabilizing secondary orbital interactions between the fluoroalkyl ligand and the Pd center and that enhancement of these interactions is one reason why complexes containing hemilabile or monodentate ligands generate catalysts that are particularly active for the coupling of aryl halides with partially fluorinated alkyl groups.

**Effect of the Electronic Properties of the Pd-Bound Aryl Ligand.** Finally, to conduct a systematic study of the effect of the electronic properties of the palladium-bound aryl group that couples with the fluoroalkyl group during reductive elimination from *cis*-**Pd-$R^F$** complexes, we computed the barriers to reductive elimination from a set of complexes with varying substituents on the palladium-bound aryl group (eq 5). We obtained the lowest-energy ground-state,

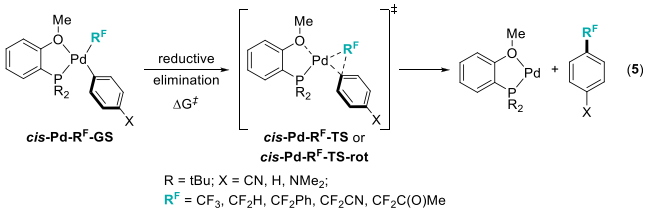


(5)

transition-state, and rotated transition-state structures of a representative series of *cis*-**Pd-$R^F$** complexes ($R^F$ = $CF_3$, $CF_2H$, $CF_2CN$, $CF_2Ph$, and $CF_2C(O)Me$) that contained electron-poor 4-cyanophenyl or electron-rich 4-(dimethylamino)phenyl ligands and compared the computed barriers to reductive elimination from these complexes to those from *cis*-**Pd-$R^F$** complexes containing unsubstituted phenyl ligands (Table 6). For complexes containing $R^F$ ligands that can participate in secondary orbital interactions, i.e., $R^F$ = $CF_2H$, $CF_2CN$, $CF_2Ph$, and $CF_2C(O)Me$, the barriers to reductive elimination from species containing the more electron-donating 4-(dimethylamino)phenyl ligand were lower than the barriers for those containing the less electron-rich phenyl or 4-

**Table 6. Free Energy Barriers to Reductive Elimination ($\Delta G^{\ddagger}$) from Transition-State Structures Containing Unsubstituted or *para*-Substituted Phenyl Groups**

| | | $\Delta G^{\ddagger}$ (kcal/mol) | | |
|---|---|---|---|---|
| entry | transition-state structure | *p*-CN | *p*-H | *p*-$NMe_2$ |
| 1 | *cis*-**Pd-$CF_2H$-TS** | 19.0 | 18.5 | 17.5 |
| 2 | *cis*-**Pd-$CF_2CN$-TS** | 22.5 | 21.0 | 19.2 |
| 3 | *cis*-**Pd-$CF_2Ph$-TS** | 18.7 | 17.3 | 16.9 |
| 4 | *cis*-**Pd-$CF_2C(O)Me$-TS** | 21.6 | 21.6 | 20.3 |
| 5 | *cis*-**Pd-$CF_3$-TS** | 27.2 | 28.2 | 27.3 |
| 6 | *cis*-**Pd-$CF_2H$-TS-rot** | 24.3 | 25.1 | 25.2 |
| 7 | *cis*-**Pd-$CF_2CN$-TS-rot** | 32.2 | 33.1 | 31.5 |
| 8 | *cis*-**Pd-$CF_2Ph$-TS-rot** | 27.7 | 28.4 | 27.8 |
| 9 | *cis*-**Pd-$CF_2C(O)Me$-TS-rot** | 30.3 | 30.7 | 30.2 |


https://doi.org/10.1021/acscatal.3c02648
ACS Catal. 2023, 13, 12810−12825

cyanophenyl ligands (see entries 1−4 in Table 6). This trend matches that observed experimentally for bisphosphine-ligated arylpalladium fluoroenolate and difluoromethyl complexes[12,15,30] but is the *opposite* of that commonly observed for the reductive elimination of nonfluorinated alkylarenes and biaryls from Pd centers. Most commonly, the barriers to reductive elimination from complexes containing more electron-poor aryl ligands are lower than those from complexes containing more electron-rich aryl ligands.[16,52−54,63]

This unusual electronic effect on reductive elimination from *cis*-**Pd-R$^F$** complexes for which the transition states contain secondary orbital interactions was absent when the elimination from complexes lacked such secondary orbital interactions. No consistent trend was observed between the $\Delta G^{\ddagger}$ values for reductive elimination from complexes that lack the secondary orbital interactions (*cis*-**Pd-CF$_3$-TS** and all *cis*-**Pd-R$^F$-TS-rot**) and the electronic properties of the palladium-bound aryl group (entries 5−9, Table 6). We note that previous experimental and computational studies investigating the rates of reductive elimination from several aryl-(trifluoromethyl)palladium complexes also revealed no systematic effect of the electronic properties of the palladium-bound aryl group on the barriers to reductive elimination of trifluoromethylarenes.[18,72]

We propose that the greater electron density on the Pd center in the transition states *cis*-**Pd-R$^F$-TS** of complexes containing the more electron-donating 4-(dimethylamino)-phenyl ligand enhances the stabilizing donor−acceptor interaction between d(Pd) orbitals and the $\pi^*$ orbital of the unsaturated group or the $\sigma^*$ orbital of the $\alpha$-C−H bond of the R$^F$ ligand. This enhanced stabilizing secondary orbital interaction results in a lower barrier to reductive elimination. However, the electron density around Pd resulting from the electron-donating ability of the phenyl ligand has less impact on the barrier to reductive elimination for complexes undergoing reductive elimination through transition states *cis*-**Pd-CF$_3$-TS** and all *cis*-**Pd-R$^F$-TS-rot** that lack the donor−acceptor interaction.

## CONCLUSION

In-depth DFT calculations investigating the effect of the fluoroalkyl ligand on the barrier to reductive elimination from (**L**)Pd(aryl)(fluoroalkyl) (**L** = di-*tert*-butyl(2-methoxyphenyl)-phosphine) complexes to form fluoroalkylarenes have revealed the strong influence of secondary orbital interactions between the metal and the substituents in the fluoroalkyl ligand on the barriers to reductive elimination. The energies of ground-state and transition-state structures in which the fluoroalkyl group is *cis*- to the methoxy fragment of ligand **L** are generally lower than those for structures in which the fluoroalkyl group is *trans*- to the methoxy fragment. A descriptor Q(R$^F$), defined as the sum of QTAIM atomic charges of the fluoroalkyl (R$^F$) fragment in the ground-state structure *cis*-**Pd-R$^F$-GS**, was developed to describe the electron-withdrawing ability of the R$^F$ ligand quantitatively and correlated strongly with the barrier to reductive elimination in the absence of the secondary orbital interactions. The barriers to reductive elimination from complexes containing more electron-withdrawing fluoroalkyl ligands are generally higher than those containing less electron-withdrawing fluoroalkyl ligands in the absence of this secondary orbital interaction.

However, analyses of the lowest-energy transition-state structures *cis*-**Pd-R$^F$-GS-TS** by IGMH, NBO, and Wiberg bond index analyses revealed the presence of stabilizing secondary orbital interactions between the Pd center and the $\alpha$-$\pi$-acceptors or the $\alpha$-hydrogens in the R$^F$ fragment in the transition states that were absent in the ground states. These secondary orbital interactions exist in the transition states because (1) the methoxy fragment of the ligand **L** dissociates from Pd and opens a free coordination site, (2) the distance between Pd and the $\pi$-acceptor or the $\alpha$-hydrogen in the migrating fluoroalkyl ligand is short, and (3) the substituent in the R$^F$ ligand and the metal center are coplanar in the transition states. The magnitude of such stabilization was estimated to be 4.7−9.9 kcal/mol, and this stabilization accounts for the much lower barriers to reductive elimination from arylpalladium difluoroenolates, difluorocyanomethyl, difluorobenzyl, and difluoromethyl complexes compared to perfluoroalkyl complexes. These secondary interactions account for the poor correlation between the experimental rates of reductive elimination from palladium(aryl)-(fluoroalkyl) complexes and common parameters of the fluoroalkyl ligands (e.g., steric or electronic properties). In the absence of these interactions, computed barriers to reductive elimination correlate linearly with the electronic properties of the fluoroalkyl ligands. Finally, the barrier to reductive elimination from a palladium complex containing a more electron-donating aryl ligand that couples with the fluoroalkyl fragment in the transition state is lower than that from a palladium complex containing a less electron-donating aryl ligand if the fluoroalkyl ligand can participate in stabilizing secondary orbital interactions with Pd in the transition state because such stabilizations are enhanced by a more electron-rich metal center. This work rationalizes the scope and effects of ancillary ligands on a wide range of coupling reactions involving fluoroalkyl ligands and can facilitate future development of novel Pd-catalyzed fluoroalkylations of aryl halides.

## ASSOCIATED CONTENT

### Supporting Information

The Supporting Information is available free of charge at https://pubs.acs.org/doi/10.1021/acscatal.3c02648.

Computational methods, geometries and energies of optimized structures, and details of calculations (PDF)

Atomic coordinates of optimized structures (XYZ)

## AUTHOR INFORMATION


### Corresponding Author

**John F. Hartwig** − *Department of Chemistry, University of California, Berkeley, California 94720, United States;* orcid.org/0000-0002-4157-468X; Email: jhartwig@berkeley.edu

### Authors

**Eric D. Kalkman** − *Department of Chemistry, University of California, Berkeley, California 94720, United States;* orcid.org/0000-0002-9365-1261

**Yehao Qiu** − *Department of Chemistry, University of California, Berkeley, California 94720, United States;* orcid.org/0000-0002-2650-0703

Complete contact information is available at: https://pubs.acs.org/10.1021/acscatal.3c02648

### Author Contributions

†E.D.K. and Y.Q. contributed equally to this work. The manuscript was written through contributions of all authors. All authors have given approval to the final version of the manuscript.

### Notes

The authors declare no competing financial interest.

## ■ ACKNOWLEDGMENTS

We thank the NSF (CHE-1955635) for support of this work. We gratefully acknowledge the Molecular Graphics and Computation Facility (MGCF) at the University of California, Berkeley, which is supported by NIH S10OD023532, for its assistance in this work. Y.Q. and E.D.K. thank Nicholas Hadler for assistance with some calculations.

## ■ REFERENCES

(1) Böhm, H.-J.; Banner, D.; Bendels, S.; Kansy, M.; Kuhn, B.; Müller, K.; Obst-Sander, U.; Stahl, M. Fluorine in Medicinal Chemistry. *ChemBioChem.* **2004**, *5*, 637−643.
(2) Dolbier, W. R. Fluorine chemistry at the millennium. *J. Fluorine Chem.* **2005**, *126*, 157−163.
(3) Gillis, E. P.; Eastman, K. J.; Hill, M. D.; Donnelly, D. J.; Meanwell, N. A. Applications of Fluorine in Medicinal Chemistry. *J. Med. Chem.* **2015**, *58*, 8315−8359.
(4) Inoue, M.; Sumii, Y.; Shibata, N. Contribution of Organofluorine Compounds to Pharmaceuticals. *ACS Omega* **2020**, *5*, 10633−10640.
(5) Jeschke, P. The Unique Role of Fluorine in the Design of Active Ingredients for Modern Crop Protection. *ChemBioChem.* **2004**, *5*, 570−589.
(6) Meanwell, N. A. Synopsis of Some Recent Tactical Application of Bioisosteres in Drug Design. *J. Med. Chem.* **2011**, *54*, 2529−2591.
(7) Purser, S.; Moore, P. R.; Swallow, S.; Gouverneur, V. Fluorine in medicinal chemistry. *Chem. Soc. Rev.* **2008**, *37*, 320−330.
(8) Wang, J.; Sánchez-Roselló, M.; Aceña, J. L.; del Pozo, C.; Sorochinsky, A. E.; Fustero, S.; Soloshonok, V. A.; Liu, H. Fluorine in Pharmaceutical Industry: Fluorine-Containing Drugs Introduced to the Market in the Last Decade (2001−2011). *Chem. Rev.* **2014**, *114*, 2432−2506.
(9) Yamazaki, T. T.; Taguchi, T.; Ojima, I. Unique Properties of Fluorine and Their Relevance to Medicinal Chemistry and Chemical Biology. In *Fluorine in Medicinal Chemistry and Chemical Biology*; John Wiley & Sons, Ltd, 2009; pp 1−49.
(10) Kirk, K. L. Fluorination in Medicinal Chemistry: Methods, Strategies, and Recent Developments. *Org. Process Res. Dev.* **2008**, *12*, 305−321.
(11) Albéniz, A. C.; Casares, J. A. Palladium-Mediated Organofluorine Chemistry. *Adv. Organomet. Chem.* **2014**, *62*, 1−110.
(12) Kalkman, E. D.; Hartwig, J. F. Direct Observation of Diastereomeric α-C-Bound Enolates during Enantioselective α-Arylations: Synthesis, Characterization, and Reactivity of Arylpalladium Fluorooxindole Complexes. *J. Am. Chem. Soc.* **2021**, *143*, 11741−11750.
(13) Lalloo, N.; Malapit, C. A.; Taimoory, S. M.; Brigham, C. E.; Sanford, M. S. Decarbonylative Fluoroalkylation at Palladium(II): From Fundamental Organometallic Studies to Catalysis. *J. Am. Chem. Soc.* **2021**, *143*, 18617−18625.
(14) Hughes, R. P. Organo-Transition Metal Compounds Containing Perfluorinated Ligands. *Adv. Organomet. Chem.* **1990**, *31*, 183−267.
(15) Arlow, S. I.; Hartwig, J. F. Synthesis, Characterization, and Reactivity of Palladium Fluoroenolate Complexes. *J. Am. Chem. Soc.* **2017**, *139*, 16088−16091.
(16) Culkin, D. A.; Hartwig, J. F. Carbon-Carbon Bond-Forming Reductive Elimination from Arylpalladium Complexes Containing Functionalized Alkyl Groups. Influence of Ligand Steric and Electronic Properties on Structure, Stability, and Reactivity. *Organometallics* **2004**, *23*, 3398−3416.
(17) Bakhmutov, V. I.; Bozoglian, F.; Gómez, K.; González, G.; Grushin, V. V.; Macgregor, S. A.; Martin, E.; Miloserdov, F. M.; Novikov, M. A.; Panetier, J. A.; Romashov, L. V. CF3-Ph Reductive Elimination from [(Xantphos)Pd(CF3)(Ph)]. *Organometallics* **2012**, *31*, 1315−1328.
(18) Cho, E. J.; Senecal, T. D.; Kinzel, T.; Zhang, Y.; Watson, D. A.; Buchwald, S. L. The Palladium-Catalyzed Trifluoromethylation of Aryl Chlorides. *Science* **2010**, *328*, 1679−1681.
(19) Ferguson, D. M.; Bour, J. R.; Canty, A. J.; Kampf, J. W.; Sanford, M. S. Stoichiometric and Catalytic Aryl-Perfluoroalkyl Coupling at Tri-tert-butylphosphine Palladium(II) Complexes. *J. Am. Chem. Soc.* **2017**, *139*, 11662−11665.
(20) Grushin, V. V.; Marshall, W. J. Facile Ar-CF3 Bond Formation at Pd. Strikingly Different Outcomes of Reductive Elimination from [(Ph3P)2Pd(CF3)Ph] and [(Xantphos)Pd(CF3)Ph]. *J. Am. Chem. Soc.* **2006**, *128*, 12644−12645.
(21) Grushin, V. V.; Marshall, W. J. Unexpected H2O-Induced Ar-X Activation with Trifluoromethylpalladium(II) Aryls. *J. Am. Chem. Soc.* **2006**, *128*, 4632−4641.
(22) Maleckis, A.; Sanford, M. S. Catalytic Cycle for Palladium-Catalyzed Decarbonylative Trifluoromethylation using Trifluoroacetic Esters as the CF3 Source. *Organometallics* **2014**, *33*, 2653−2660.
(23) Maleckis, A.; Sanford, M. S. Synthesis of Fluoroalkyl Palladium and Nickel Complexes via Decarbonylation of Acylmetal Species. *Organometallics* **2014**, *33*, 3831−3839.
(24) Nielsen, M. C.; Bonney, K. J.; Schoenebeck, F. Computational Ligand Design for the Reductive Elimination of ArCF3 from a Small Bite Angle PdII Complex: Remarkable Effect of a Perfluoroalkyl Phosphine. *Angew. Chem., Int. Ed.* **2014**, *53*, 5903−5906.
(25) Zhang, S.-L.; Deng, Z.-Q. Synthesis and reductive elimination of arylPd(ii) trifluoromethyl complexes: a remarkable concentration effect on chemoselectivity. *Phys. Chem. Chem. Phys.* **2016**, *18*, 32664−32667.
(26) Anstaett, P.; Schoenebeck, F. Reductive Elimination of ArCF3 from Bidentate PdII Complexes: A Computational Study. *Chem. - Eur. J.* **2011**, *17*, 12340−12346.
(27) Arlow, S. I. *The Development of Transition Metal-Catalyzed Fluoroalkylation and Fluoroenolate Arylation Reactions*. Ph.D. Thesis, University of California, Berkeley, CA, 2018.
(28) Feng, Z.; Min, Q.-Q.; Zhang, X. Access to Difluoromethylated Arenes by Pd-Catalyzed Reaction of Arylboronic Acids with Bromodifluoroacetate. *Org. Lett.* **2016**, *18*, 44−47.
(29) Ferguson, D. M.; Bour, J. R.; Canty, A. J.; Kampf, J. W.; Sanford, M. S. Aryl-CF3 Coupling from Phosphinoferrocene-Ligated Palladium(II) Complexes. *Organometallics* **2019**, *38*, 519−526.
(30) Gu, Y.; Leng, X.; Shen, Q. Cooperative dual palladium/silver catalyst for direct difluoromethylation of aryl bromides and iodides. *Nat. Commun.* **2014**, *5*, 5405.
(31) Lu, C.; Gu, Y.; Wu, J.; Gu, Y.; Shen, Q. Palladium-catalyzed difluoromethylation of heteroaryl chlorides, bromides and iodides. *Chem. Sci.* **2017**, *8*, 4848−4852.
(32) Mormino, M. *The Development of Transition Metal-Catalyzed Fluoroalkylation Reactions of Aryl Electrophiles*. Ph.D. Thesis, University of California, Berkeley, CA, 2017.
(33) Wade Wolfe, M. M.; Shanahan, J. P.; Kampf, J. W.; Szymczak, N. K. Defluorinative Functionalization of Pd(II) Fluoroalkyl Complexes. *J. Am. Chem. Soc.* **2020**, *142*, 18698−18705.
(34) Weinhold, F.; Landis, C. R.; Glendening, E. D. What is NBO analysis and how is it useful? *Int. Rev. Phys. Chem.* **2016**, *35*, 399−440.
(35) Johnson, E. R.; Keinan, S.; Mori-Sánchez, P.; Contreras-García, J.; Cohen, A. J.; Yang, W. Revealing Noncovalent Interactions. *J. Am. Chem. Soc.* **2010**, *132*, 6498−6506.
(36) Lu, T.; Chen, Q. Independent gradient model based on Hirshfeld partition: A new method for visual study of interactions in chemical systems. *J. Comput. Chem.* **2022**, *43*, 539−555.
(37) Lefebvre, C.; Rubez, G.; Khartabil, H.; Boisson, J.-C.; Contreras-García, J.; Hénon, E. Accurately extracting the signature


https://doi.org/10.1021/acscatal.3c02648
ACS Catal. 2023, 13, 12810−12825

of intermolecular interactions present in the NCI plot of the reduced density gradient versus electron density. *Phys. Chem. Chem. Phys.* **2017**, *19*, 17928−17936.
(38) Frisch, M. J. T.; G, W.; Schlegel, H. B.; Scuseria, G. E.; Robb, M. A.; Cheeseman, J. R.; Scalmani, G.; Barone, V.; Petersson, G. A.; Nakatsuji, H.; Li, X.; Caricato, M.; Marenich, A. V.; Bloino, J.; Janesko, B. G.; Gomperts, R.; Mennucci, B.; Hratchian, H. P.; Ortiz, J. V.; Izmaylov, A. F.; Sonnenberg, J. L.; Williams-Young, D.; Ding, F.; Lipparini, F.; Egidi, F.; Goings, J.; Peng, B.; Petrone, A.; Henderson, T.; Ranasinghe, D.; Zakrzewski, V. G.; Gao, J.; Rega, N.; Zheng, G.; Liang, W.; Hada, M.; Ehara, M.; Toyota, K.; Fukuda, R.; Hasegawa, J.; Ishida, M.; Nakajima, T.; Honda, Y.; Kitao, O.; Nakai, H.; Vreven, T.; Throssell, K.; Montgomery, J. A.; Peralta, J. E.; Ogliaro, F.; Bearpark, M. J.; Heyd, J. J.; Brothers, E. N.; Kudin, K. N.; Staroverov, V. N.; Keith, T. A.; Kobayashi, R.; Normand, J.; Raghavachari, K.; Rendell, A. P.; Burant, J. C.; Iyengar, S. S.; Tomasi, J.; Cossi, M.; Millam, J. M.; Klene, M.; Adamo, C.; Cammi, R.; Ochterski, J. W.; Martin, R. L.; Morokuma, K.; Farkas, O.; Foresman, J. B.; Fox, D. J. *Gaussian 16*, rev. A.01; Gaussian, Inc.: Wallingford, CT, 2016.
(39) Perdew, J. P.; Burke, K.; Ernzerhof, M. Generalized Gradient Approximation Made Simple. *Phys. Rev. Lett.* **1996**, *77*, 3865−3868.
(40) Adamo, C.; Barone, V. Toward reliable density functional methods without adjustable parameters: The PBE0 model. *J. Chem. Phys.* **1999**, *110*, 6158−6170.
(41) Grimme, S.; Ehrlich, S.; Goerigk, L. Effect of the damping function in dispersion corrected density functional theory. *J. Comput. Chem.* **2011**, *32*, 1456−1465.
(42) Zheng, J.; Xu, X.; Truhlar, D. G. Minimally augmented Karlsruhe basis sets. *Theor. Chem. Acc.* **2011**, *128*, 295−305.
(43) Marenich, A. V.; Cramer, C. J.; Truhlar, D. G. Universal Solvation Model Based on Solute Electron Density and on a Continuum Model of the Solvent Defined by the Bulk Dielectric Constant and Atomic Surface Tensions. *J. Phys. Chem. B* **2009**, *113*, 6378−6396.
(44) Dohm, S.; Hansen, A.; Steinmetz, M.; Grimme, S.; Checinski, M. P. Comprehensive Thermochemical Benchmark Set of Realistic Closed-Shell Metal Organic Reactions. *J. Chem. Theory Comput.* **2018**, *14*, 2596−2608.
(45) Iron, M. A.; Janes, T. Evaluating Transition Metal Barrier Heights with the Latest Density Functional Theory Exchange-Correlation Functionals: The MOBH35 Benchmark Database. *J. Phys. Chem. A* **2019**, *123*, 3761−3781.
(46) Iron, M. A.; Janes, T. Correction to "Evaluating Transition Metal Barrier Heights with the Latest Density Functional Theory Exchange-Correlation Functionals: The MOBH35 Benchmark Database. *J. Phys. Chem. A* **2019**, *123*, 6379−6380.
(47) Choi, K.; Mormino, M. G.; Kalkman, E. D.; Park, J.; Hartwig, J. F. Palladium-Catalyzed Aryldifluoromethylation of Aryl Halides with Aryldifluoromethyl Trimethylsilanes. *Angew. Chem., Int. Ed.* **2022**, *61*, No. e202208204.
(48) Pan, F.; Boursalian, G. B.; Ritter, T. Palladium-Catalyzed Decarbonylative Difluoromethylation of Acid Chlorides at Room Temperature. *Angew. Chem., Int. Ed.* **2018**, *57*, 16871−16876.
(49) Peacock, D. M.; Jiang, Q.; Cundari, T. R.; Hartwig, J. F. Reductive Elimination to Form C(sp3)-N Bonds from Palladium(II) Primary Alkyl Complexes. *Organometallics* **2018**, *37*, 3243−3247.
(50) Peacock, D. M.; Jiang, Q.; Hanley, P. S.; Cundari, T. R.; Hartwig, J. F. Reductive Elimination from Phosphine-Ligated Alkylpalladium(II) Amido Complexes To Form sp3 Carbon-Nitrogen Bonds. *J. Am. Chem. Soc.* **2018**, *140*, 4893−4904.
(51) To enable comparisons among different fluoroalkyl ligands, we only considered the energetic barriers to reductive elimination from *cis*-**Pd-R$^F$** structures, as in most cases the *cis* isomers were the lower-energy structures.
(52) Mann, G.; Baranano, D.; Hartwig, J. F.; Rheingold, A. L.; Guzei, I. A. Carbon-Sulfur Bond-Forming Reductive Elimination Involving sp-, sp2-, and sp3-Hybridized Carbon. Mechanism, Steric Effects, and Electronic Effects on Sulfide Formation. *J. Am. Chem. Soc.* **1998**, *120*, 9205−9219.
(53) Driver, M. S.; Hartwig, J. F. Carbon-Nitrogen-Bond-Forming Reductive Elimination of Arylamines from Palladium(II) Phosphine Complexes. *J. Am. Chem. Soc.* **1997**, *119*, 8232−8245.
(54) Widenhoefer, R. A.; Buchwald, S. L. Electronic Dependence of C-O Reductive Elimination from Palladium (Aryl)neopentoxide Complexes. *J. Am. Chem. Soc.* **1998**, *120*, 6504−6511.
(55) Widenhoefer, R. A.; Zhong, H. A.; Buchwald, S. L. Direct Observation of C-O Reductive Elimination from Palladium Aryl Alkoxide Complexes To Form Aryl Ethers. *J. Am. Chem. Soc.* **1997**, *119*, 6787−6795.
(56) Bader, R. F. W. Atoms in molecules. *Acc. Chem. Res.* **1985**, *18*, 9−15.
(57) We also investigated orbital-population-based methods for determining atomic charges, such as NBO (see ref 33) and intrinsic atomic orbitals (IAO); however, these methods did not provide consistent correlations with energy barriers (see the Supporting Information for details).
(58) A less computationally expensive descriptor, Q′(R$^F$), based on the QTAIM charges of the R$^F$ fragments of the fluoroalkylbenzenes **Ph-R$^F$** was found to correlate linearly with Q(R$^F$) ($R^2$ = 0.87). Substituting Q′(R$^F$) for Q(R$^F$) in the subsequent analyses affords similar conclusions to those obtained from the analyses with Q(R$^F$) presented in the main text. For a more detailed comparison of these two descriptors, see section 3 of the Supporting Information.
(59) Hansch, C.; Leo, A.; Taft, R. W. A survey of Hammett substituent constants and resonance and field parameters. *Chem. Rev.* **1991**, *91*, 165−195.
(60) Because the fluoroalkyl groups are necessarily saturated at the point of connection, resonance effects are absent between the fluoroalkyl group and the rest of the molecule, or between the X fragment of $CF_2X$ and the $CF_2$ fragment. Therefore, the electronic effect of the R$^F$ fragment should be chiefly inductive and well represented by $\sigma_m$.
(61) Culkin, D. A.; Hartwig, J. F. C-C Bond-Forming Reductive Elimination of Ketones, Esters, and Amides from Isolated Arylpalladium(II) Enolates. *J. Am. Chem. Soc.* **2001**, *123*, 5816−5817.
(62) Culkin, D. A.; Hartwig, J. F. Palladium-Catalyzed $\alpha$-Arylation of Carbonyl Compounds and Nitriles. *Acc. Chem. Res.* **2003**, *36*, 234−245.
(63) Hartwig, J. F. Electronic Effects on Reductive Elimination To Form Carbon-Carbon and Carbon-Heteroatom Bonds from Palladium(II) Complexes. *Inorg. Chem.* **2007**, *46*, 1936−1947.
(64) Canty, A. J. Development of organopalladium(IV) chemistry: fundamental aspects and systems for studies of mechanism in organometallic chemistry and catalysis. *Acc. Chem. Res.* **1992**, *25*, 83−90.
(65) Roy, S.; Puddephatt, R. J.; Scott, J. D. Mechanism and energetics of reductive elimination of ethane from some tetramethylplatinum(IV) complexes. *J. Chem. Soc., Dalton Trans.* **1989**, 2121−2125.
(66) Crabtree, R. H. Transition Metal Complexation of $\sigma$ Bonds. *Angew. Chem., Int. Ed. Engl.* **1993**, *32*, 789−805.
(67) Low, J. J.; Goddard, W. A. Theoretical studies of oxidative addition and reductive elimination. 2. Reductive coupling of hydrogen-hydrogen, hydrogen-carbon, and carbon-carbon bonds from palladium and platinum complexes. *Organometallics* **1986**, *5*, 609−622.
(68) Wiberg, K. B. Application of the pople-santry-segal CNDO method to the cyclopropylcarbinyl and cyclobutyl cation and to bicyclobutane. *Tetrahedron* **1968**, *24*, 1083−1096.
(69) Bondi, A. van der Waals Volumes and Radii. *J. Phys. Chem.* **1964**, *68*, 441−451.
(70) The $\Delta E_{se}$ value does not monotonically increase with the volume of the R$^F$ ligand, possibly because the different spatial distributions of the R$^F$ ligands lead to errors in the DFT method.
(71) Hartwig, J. F. *Organotransition Metal Chemistry: From Bonding to Catalysis*. University Science Books: Melville, NY, 2010; p 323−324.


https://doi.org/10.1021/acscatal.3c02648
*ACS Catal.* 2023, 13, 12810−12825

(72) Zhang, S.-L.; Huang, L.; Sun, L.-J. The mechanism, electronic and ligand effects for reductive elimination from arylPd(ii) trifluoromethyl complexes: a systematic DFT study. *Dalton Trans.* **2015**, *44*, 4613−4622.



https://doi.org/10.1021/acscatal.3c02648
*ACS Catal.* 2023, 13, 12810−12825